Journal of Inorganic Biochemistry 227 (2022) 111687

Contents lists available at ScienceDirect

Journal of Inorganic Biochemistry

journal homepage: www.elsevier.com/locate/jinorgbio

Review Article

Sulfide and transition metals - A partnership for life

Biplab K. Maiti [a], Luisa B. Maia [b], José J.G. Moura [b,*]

[a] National Institute of Technology Sikkim, Department of Chemistry, Ravangla Campus, Barfung Block, Ravangla Sub Division, South Sikkim 737139, India
[b] LAQV, REQUIMTE, Department of Chemistry, NOVA School of Science and Technology (FCT NOVA), Universidade NOVA de Lisboa, Campus de Caparica, Portugal

ARTICLE INFO

Keywords:
Sulfide
Metal-sulfides
Metalloproteins
Coordination modes
Catalysis
Inhibitor

ABSTRACT

Sulfide and transition metals often came together in Biology. The variety of possible structural combinations enabled living organisms to evolve an array of highly versatile metal-sulfide centers to fulfill different physiological roles. The ubiquitous iron-sulfur centers, with their structural, redox, and functional diversity, are certainly the best-known partners, but other metal-sulfide centers, involving copper, nickel, molybdenum or tungsten, are equally crucial for Life. This review provides a concise overview of the exclusive sulfide properties as a metal ligand, with emphasis on the structural aspects and biosynthesis. Sulfide as catalyst and as a substrate is discussed. Different enzymes are considered, including xanthine oxidase, formate dehydrogenases, nitrogenases and carbon monoxide dehydrogenases. The sulfide effect on the activity and function of iron-sulfur, heme and zinc proteins is also addressed.

1. Introduction

Sulfide (S^{2-}) is a strong nucleophile [1] that can bind several transition metal ions, giving rise to a variety of metal-sulfide centers (M/S) of different compositions and structures, covering terminal, and bridging μ_2-S, μ_3-S and μ_4-S arrangements. Living organisms learned to exploit this rich chemistry in a wide range of biochemical processes, from metal storage and regulation/sensing to electron transfer and catalysis [2–8]. Striking examples of the chemical versatility of M/S clusters are provided by nitrogenases (cleavage of N—N bonds) [9–11], nitrous oxide reductase (cleavage of N—O) [12,13], carbon monoxide dehydrogenases (CODH; cleavage of C—O) [14–17], xanthine oxidase (XO; cleavage of C—H coupled with C—O bond formation) [14,15], formate dehydrogenases (FDH; cleavage and formation of C—H) [18,19], and orange protein (ORP) [20,21]. The chemical repertoire of M/S includes also intramolecular and intermolecular electron transfer, as can be illustrated by numerous iron-sulfur (Fe/S) center-containing proteins harboring [2Fe—2S], [3Fe—4S] and [4Fe-4S] centers [3,22–26]. These centers are also crucial building-block units of the more complex structures present in the active site of key enzymes such

Abbreviations: 5-dAdo, 5-deoxyadenosyl radical; ABA3, plant molybdenum cofactor sulfurase (from the biosynthesis of abscisic acid); ACE, angiotensin converting enzyme; ACE2, angiotensin converting enzyme 2; AR, androgen receptor; ATP, adenosine triphosphate; BioB, biotin synthase; CBS, cystathionine β-synthase; CcO, cytochrome *c* oxidase; CODH, carbon monoxide dehydrogenase (both types); CODHCh, CODH from *Carboxydothermus hydrogenoformans*; CODHMt, CODH from *Moorella thermoacetica*; CODHRr, CODH from *Rhodospirillum rubrum*; cPMP, cyclic pyranopterin monophosphate; CSE, γ-cystathionase; Cu/S, copper-sulfur center(s); Cys-Mo-FDH, cysteine and molybdenum-dependent FDH; Cys-W-FDH, cysteine and tungsten-dependent FDH; DTB, dethiobiotin; DMSOR, dimethylsulfoxide reductase; DT, dithionite; eukNaR, eukaryotic nitrate reductase; Fd, ferredoxin; FDH, formate dehydrogenase(s) (both types); Feco, iron only-containing cofactor of nitrogenase active site; FeMoco, iron and molybdenum-containing cofactor of nitrogenase active site; Fe/S, iron-sulfur center(s); FeVco, iron and vanadium-containing cofactor of nitrogenase active site; FMFDH, both molybdenum- and tungsten-dependent *N*-formyl-methanofuran dehydrogenases; GSH, Glutathione; HCP, hybrid cluster-containing protein; Hb, hemoglobin; HMCS, human molybdenum cofactor sulfurase; Isc, iron sulfur cluster; Mb, myoglobin; Mo-PMN, molybdenum-coordinated pyranopterin mononucleotide; M/S, metal-sulfide center(s); MST, mercaptopyruvate sulfurtransferase; Mo,Cu/S, molybdenum and copper- sulfur center(s); Mo,Cu-CODH, molybdenum and copper-containing carbon monoxide dehydrogenase; Mo-FDH, molybdenum-dependent FDH; Mo,Fe/S, molybdenum and iron-sulfur center(s); MorP, Mo/Fe protein; MTs, metallothioneins; NaR, nitrate reductase; NHE, Normal Hydrogen Electrode potential; Nif, nitrogen fixation; N_2OR, nitrous oxide reductase; Ni,Fe-CODH, nickel and iron-containing carbon monoxide dehydrogenase; PCD, pyranopterin cytidine dinucleotide; PDT, pyranopterin dithiolene; PGD, pyranopterin guanosine dinucleotide; PLP, pyridoxal 5′-phosphate; PMN, pyranopterin mononucleotide; ORP, orange protein; SAM/AdoMet, S-adenosyl-L-methionine; SARS-CoV-2, severe acute respiratory syndrome coronavirus 2; SeCys-Mo-FDH, selenocysteine and molybdenum-dependent FDH; SeCys-W-FDH, selenocysteine and tungsten-dependent FDH; Suf, sulfur formation; XO, xanthine oxidase; W-FDH, tungsten-dependent FDH; ZF, zinc-finger.

* Corresponding author.
E-mail addresses: biplab@nitsikkim.ac.in (B.K. Maiti), luisa.maia@fct.unl.pt (L.B. Maia), jose.moura@fct.unl.pt (J.J.G. Moura).

https://doi.org/10.1016/j.jinorgbio.2021.111687
Received 3 August 2021; Received in revised form 24 November 2021; Accepted 28 November 2021
Available online 5 December 2021

as nitrogenases, nickel and iron-containing carbon monoxide dehydrogenase (Ni,Fe-CODH) [16–17] and hybrid cluster-containing protein (HCP) [27–29].

This concise review aims to showcase the diversity and versatility of M/S-containing proteins, focusing on structural and catalytic aspects of sulfide as a ligand. XO, FDH, molybdenum and copper-containing CODH (Mo,Cu-CODH), Ni,Fe-CODH and Fe/S protein will be highlighted. The role of H_2S as inhibitor or substrate in selected enzymes will be also described.

2. Overview of sulfide as a ligand

The simplest form of thiol is hydrogen sulfide (H_2S). H_2S is a colorless gas and a weak acid that exists in aqueous solution in equilibrium with two anionic conjugated bases, hydrosulfide (HS^-) and sulfide (S^{2-}), according to $pK_{a1} \sim 7.0$ and $pK_{a2} \sim 19.0$, at 25 °C [30,31]. Under physiological conditions, pH ~ 7.4, H_2S exists mainly as HS^- rather than S^{2-} ion. H_2S is the lowest oxidation state (−2) of sulfur that covers a wide variety of oxidation states such as: −2 (H_2S), 0 (S_8), +2 (SO), +4 (SO_3^{2-}) and + 6 (SO_4^{2-}). Therefore, H_2S acts as a reducing species, showing a concerted two-electron reduction potential of −0.23 V vs. NHE at pH ~ 7.0, for HS^-/S^0 redox couple [32,33]. The value is very close to the biologically relevant reduction potential value of glutathione disulfide ($E^{\circ}_{GSSG/GSH} = -0.24$ V vs. NHE [34]), and cysteine ($E^{\circ}_{cystine/cysteine} = -0.24$ V [32,35,36]). Furthermore, H_2S can be one-electron oxidized to yield the sulfide radical, showing a reduction potential of +0.92 V vs. NHE at pH ~ 7 for $E^{\circ}(S^{\bullet}, H^+/HS^-)$ redox couple [33], which is also comparable with cysteine ($E^{\circ}(RS^{\bullet}, H^+/RSH) = +0.9$ V vs. NHE) [37]. The S—H bond dissociation energy of H_2S is ~90 kcal/mol [38], similar to the S—H bond dissociation energy of thiols (92.0 ± 1.0 kcal/mol [39]). Like thiolate (RS^-), HS^- also acts as a strong nucleophile [40].

Sulfide can coordinate a wide range of metal ions to form different mononuclear to polynuclear M/S species, through a variety of terminal and μ_2-S, μ_3-S and μ_4-S bridging binding modes (Fig. 1). The interaction between simple metal salts with H_2S, in aqueous medium, produces M/S, which are often highly insoluble compounds and difficult to characterize, including MnS ($K_{sp} = 7.0 \times 10^{-19}$), FeS ($4.0 \times 10^{-19}$), NiS ($3.0 \times 10^{-21}$), ZnS ($1.6 \times 10^{-23}$), CuS ($8.0 \times 10^{-37}$), and Cu_2S (1.2×10^{-49}) [41]. However, in biological media, the protein environment prevents the formation of insoluble M/S species and allows the build-up of a variety of M/S clusters. However, the strong M-S bonds can be cleaved by strong acids (what is called acid labile sulfide), yielding H_2S gas and free metal ions. This phenomenon allows the Fe/S centers to be hydrolyzed from the respective proteins and to be, subsequently, self-assembled (or interconverted between different metals) from simple Fe^{2+} and S^{2-}, as was comprehensively described [26,42,43].

3. Metal-sulfide-containing proteins

M/S centers can be classified as mono-, homopoly- and heteropolynuclear sites, with sulfur binding to one, two, three or four metal ions, through terminal and/or bridged modes (Fig. 1).

3.1. Mononuclear sites with a terminal S binding mode

Compared to the widespread occurrence of Fe/S centers (described below), proteins harboring a metal-bound terminal sulfur are less common. Yet, the molybdenum and tungsten-containing enzymes provide several examples of this binding mode. These enzymes can be organized into two groups, in line with the metal present in the active site [15]: the molybdoenzymes [14,15] and the tungstoenzymes [44] (*note that the molybdenum-containing nitrogenase belongs to a third group of these enzymes; nitrogenases are discussed in the section below*). The molybdoenzymes are further classified into three large families [45], in accordance with the structure of their active site: XO family, sulfite oxidase family and dimethylsulfoxide reductase (DMSOR) family. The XO family is characterized by having an active site (in the oxidized form) with one molybdenum ion coordinated by the *cis*-dithiolene (–S–C=C–S–) group of one pyranopterin cofactor molecule, two oxido ligands (one axial, $Mo^{6+} = O$, and one equatorial, Mo^{6+}-OH) and a terminal sulfido group ($Mo^{6+} = S$), in a square-pyramidal geometry (Fig. 2 A, exemplified with mammalian XO) [14,15,46]. This large family has members in all forms of life, from prokaryotes to higher plants and mammals, and comprises enzymes of diverse functions such as mammalian XO and aldehyde oxidase or bacterial hydroxybenzoyl-CoA redutase and quinoline 2-oxidoreductase. The DMSOR family, that comprises only prokaryotic enzymes, is characterized by having an active site with one molybdenum ion coordinated by the *cis*-dithiolene group of two pyranopterin cofactor molecules in a trigonal prismatic geometry completed by oxygen and/or sulfur and/or selenium atoms in diverse arrangements [14,15,47,48]. Some members of this family possess a terminal sulfido group. FDHs are the best characterized ones, with an active site (in the oxidized form) with a molybdenum ion coordinated by two pyranopterin cofactor molecules, one cysteine or selenocysteine residue (Mo^{6+}-S(Cys) or Mo^{6+}-Se(Cys)) and a terminal sulfido group ($Mo^{6+} = S$) [18,19,49–51]. The tungsten family comprises similar FDH enzymes, with an active site identical to the molybdenum-dependent FDH one, but harboring a tungsten ion in the place of molybdenum (Fig. 2 B).

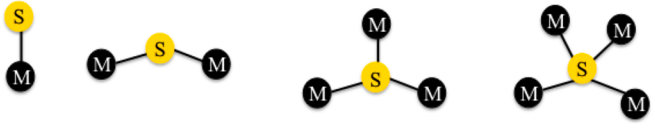

Fig. 1. Sulfur terminal and μ_2-S, μ_3-S and μ_4-S bridging binding modes in metal-sulfide centers.

3.2. Homopolynuclear sites

In this class, the most common M/S clusters are Fe/S centers, which have structural diversity, including ferredoxins containing [2Fe—2S], Rieske-[2Fe—2S], [3Fe—4S], and [4Fe-4S] cores [22–26,53]. These structures have a very rich redox chemistry and may interconvert and/or accept an extra metal atom, but all these features are out of the scope of this review (readers are refereed to [26,43,54–56] and references therein). One sulfide ligand connects two or three iron ions by μ_2-S or μ_3-S binding modes to build up [2Fe-2S], [3Fe—4S] and [4Fe-4S] respectively (Fig. 2 C and I; [3Fe—4S] not shown).

An unprecedented copper-sulfur (Cu/S) cluster is found in nitrous oxide reductase (N_2OR) [12,13,57] where one sulfide ligand connects four copper ions through a μ_4-S binding mode (Fig. 2 J), representing the highest sulfur binding mode so far found in Biology.

3.3. Heteropolynuclear sites

The molybdoenzymes, typically characterized as having a mononuclear active site center (section 3.1.), include one (so far) exception, the Mo,Cu-CODH with its hetero-binuclear active site. The *O. carboxidovorans* CODH, although classified as a XO family member, has no terminal sulfido group. Instead, its molybdenum center is coordinated to the polypeptide chain by one cysteine residue through a Mo–S–Cu–S(Cys) motif (Fig. 2 D; compare with Fig. 2 A) [58–61]. The classification of CODH as a XO family member is supported by the considerable sequence and structural homology with the bovine XO, as well as common reactivity and sensitivity to inhibition by cyanide [61–63].

A different heterometallic Mo,Cu/S center is found in ORP isolated from *D. gigas* [20,21], where a central copper ion is coordinated by two tetrathiomolydates (MoS_4^{2-}) units via two μ_2-S, with two terminal

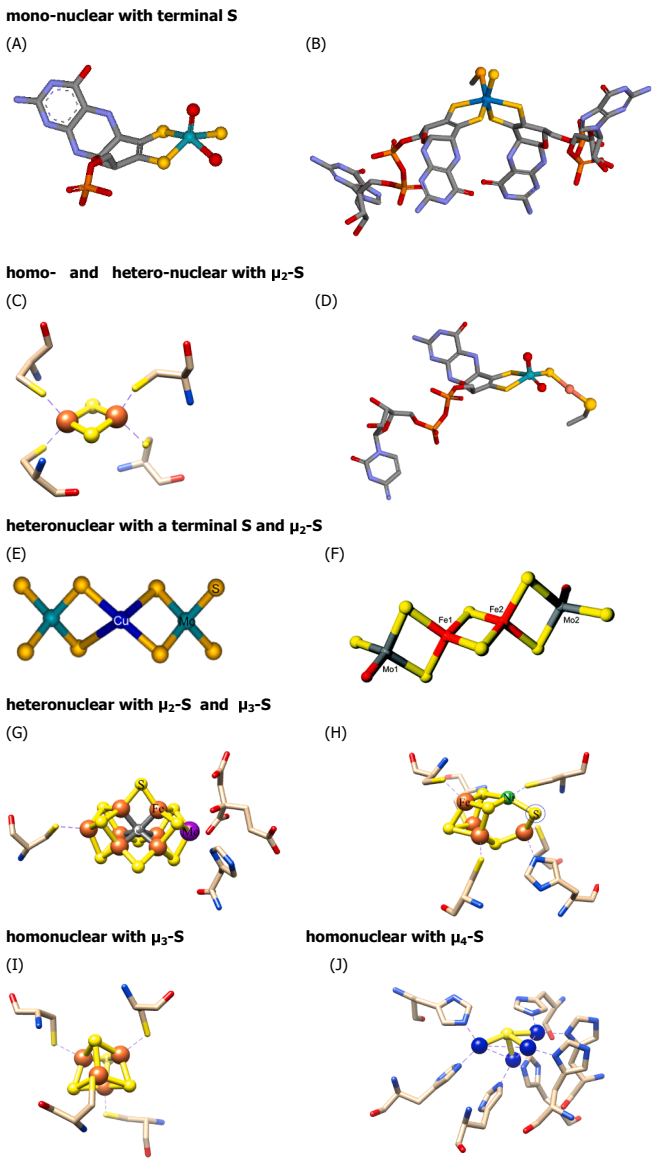

Fig. 2. Structures of representative M/S centers from selected enzymes. (A) Molybdenum center (oxidized) xanthine oxidase (bovine enzyme; structure from PDB file 1FO4); (B) tungsten center (oxidized) formate dehydrogenase (*Desulfovibrio gigas*; PDB file 1H0H); (C) [2Fe2S] ferredoxin (*Spinacia oleracea*; PDB file 1A70); (D) binuclear molybdenum and copper center of oxidized Mo, Cu-CODH (*Oligotropha carboxidovorans*; PDB file 1N5W); (E) molybdenum and copper center of orange protein (*D. gigas*; EXAFS structure [20]; (F) molybdenum and iron center of Mo/Fe protein (MorP; *Desulfovibrio alaskensis*; EXAFS structure [52]; (G) molybdenum and iron center of nitrogenase active site (*Azotobacter vinelandii* (PDB file 1M1N); (H) nickel and iron center of Ni,Fe-CODH (*Carboxydothermus hydrogenoformans*; PDB file 1SU6); (I) [4Fe4S] ferredoxin (*A. vinelandii*; PDB file 2FD2); (J) Copper center of nitrous oxide reductase active site (*Paracoccus denitrificans*; PDB file 1FWX).

sulfides (Fig. 2 E) [64]. Furthermore, a mixed molybdenum and iron-sulfur (Mo,Fe/S center) cluster is also found in Mo—Fe protein (MorP) isolated from *D. alaskensis*, where a [2Fe2S] unit is coordinated by two $MoOS_3^{2-}$ units through μ_2-S, with two terminal sulfides (Fig. 2 F) [52].

A [Mo-7Fe-9S-C] center forms the nitrogenase active site cofactor (FeMoco), a unique cluster responsible for the dinitrogen conversion into ammonia [6,9–11,65] (Fig. 2 G). The [Mo-7Fe-9S-C] cluster is formed from the combination of two cubane type subsites (with a μ_3-S binding mode), [Fe-4S-3C] and [MoFe-3S-3C] through three μ_2-S and one C ligand. It was proposed that one of the three μ_2-S ligands must be displaced to allow the dinitrogen (substrate) coordination (see nitrogenase section) [65].

In the C-cluster of CODH isolated from *C. hydrogenoformans* ($CODH_{Ch}$), [Ni-4Fe-5S], a nickel ion binds two μ_3-S ligands from the [3Fe—4S] subsite, and one μ_2-S bridges to the distal iron [66]. Herein, sulfur binds metals in μ_2-S and μ_3-S fashion (Fig. 2 H). The bridged μ_2-sulfide ion that connects the nickel to the distal iron (in *C. hydrogenoformans*) blocks the coordination of carbon monoxide (substrate) to the nickel site, thus acting as a reversible enzymatic inhibitor [66].

4. Metal-sulfide clusters biosynthesis

4.1. Iron-sulfur clusters

Synthesis of Fe/S clusters in vivo is a complex process and requires an intricate biosynthetic machinery. The sulfide is the main constituent in these clusters that is generated endogenously from cysteine by three pyridoxal 5′-phosphate (PLP)-dependent cysteine desulfurase enzymes for the biosynthesis of Fe/S cluster [67]. Cysteine desulfurases are used not only for Fe/S clusters, but also for the synthesis of a variety of other sulfur-containing biomolecules, including the molybdenum center (as discussed below), thiolated tRNA, and thiamine [68–70].

The Fe/S clusters are ubiquitous and ancient protein cofactors in biology, essential for a wide range of biological functions, such as electron transfer and enzyme catalysis, including protein synthesis, ATP, oxidative stress defense, DNA repair, and maintenance of genome integrity [71–74]. In vitro, the Fe/S clusters are spontaneously assembled in protein scaffolds upon addition of Fe^{2+} and S^{2-} ions [42,43,75]. As both free Fe and S^{2-} ions are highly toxic in vivo, the Fe—S cluster assembly is tightly regulated in biosynthetic pathways [23]. Despite the chemical simplicity of Fe/S clusters, the biosynthesis is rather complicated [76–80]. Three distinct Fe/S cluster assemble machineries for biosynthesis of Fe/S cluster in Biology have been identified: Nif (nitrogen fixation), Isc (iron sulfur cluster), and the Suf system (sulfur formation) [23,81–83]. All machineries (Nif, Isc and Suf) commonly use a key enzyme, cysteine desulfurases, NifS, IscS, and SufS, which catalyze the production of sulfur from L-cysteine for Fe/S cluster biosynthesis [23,81,83,84–86]. However, the NifS or NifS-like cysteine desulfurase enzymes are present in almost all living organisms and produce inorganic sulfide for Fe/S cluster synthesis.

Cysteine desulfurase is a PLP-dependent enzyme, which catalyzes the conversion of substrate L-cysteine to L-alanine and sulfane sulfur (S^0) (Fig. 3) [68,87,88]. The formation of sulfane sulfur is transferred to catalytic cysteine residue in proteins to form a cysteine bound protein intermediate (Cys-SSH) that is the ultimate source of sulfide ions for Fe/S cluster biogenesis [67,81,87,89]. The sulfide is produced from the persulfide intermediate by the reductive cleavage of the persulfide bond [67], and sulfide is subsequently delivered to target iron-sulfur proteins such as scaffold proteins NifU and/or IscU for finally Fe/S clusters synthesis.

The assembly of FeMoco or other mixed core structure of the cofactor

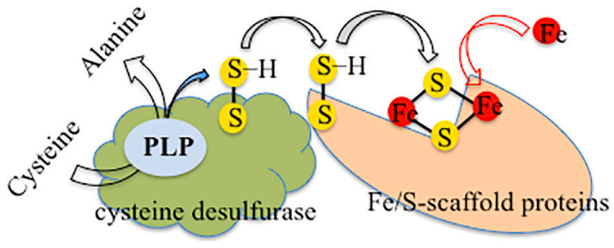

Fig. 3. Sulfide formation by PLP-dependent cysteine desulfurase and its delivery to Fe/S scaffold proteins via a persulfide intermediate.

is synthesized by NifS and NifU machineries, which mobilize Fe and S for the formation of small Fe/S building blocks [90,91].

4.2. Molybdenum centers

The biosynthesis of molybdenum cofactors shares three conserved steps in all organisms, involving the sequential conversion of 5'GTP into cyclic pyranopterin monophosphate (cPMP), pyranopterin dithiolene (PDT) and the final molybdenum insertion from molybdate to yield a molybdenum-coordinated pyranopterin mononucleotide (Mo-PMN) (Fig. 4, top) [92–102]. In prokaryotes, Mo-PMN is further modified by the addition of the nucleotides CMP or GMP to its terminal phosphate group, to form the pyranopterin cytidine dinucleotide (PCD) or pyranopterin guanosine dinucleotide (PGD) found mainly in enzymes of the XO and DMSOR families [103–110]. In the DMSOR family enzymes that possess two PGD moieties, the insertion of the second PMN moiety precedes the addition of the GMP.

For the enzymes possessing a terminal sulfido group, its insertion is the last step in the centers maturation, with sulfuration occuring prior to the molybdenum center incorporation into the enzyme. In eukaryotic

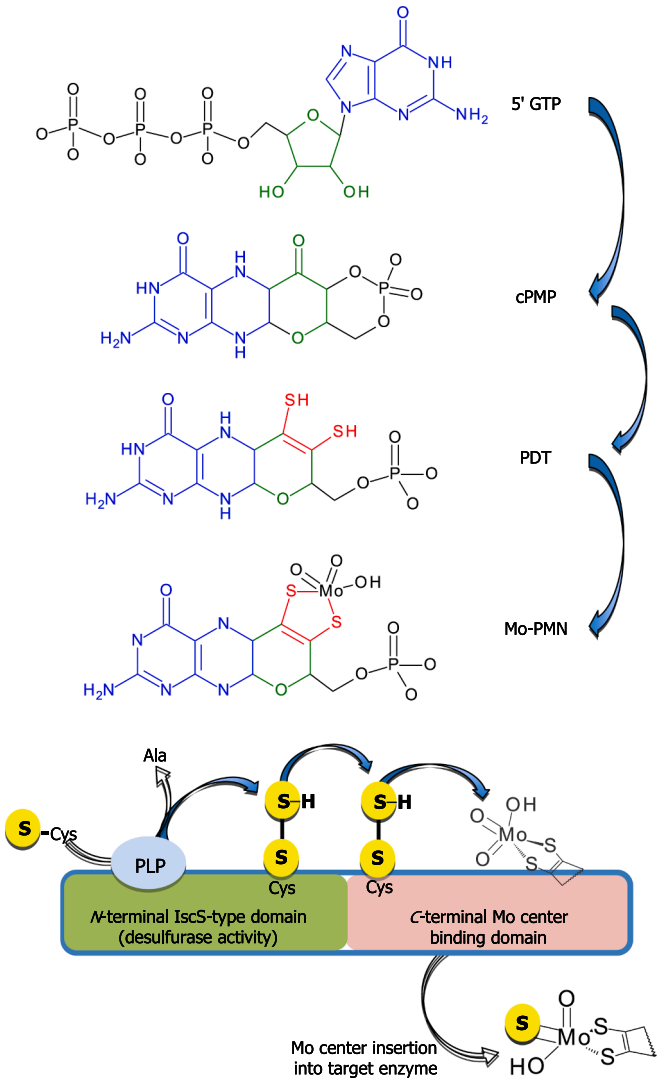

Fig. 4. Top: Molybdenum center biosynthesis pathway. Only the relevant intermediates are shown. Bottom: Proposed mechanism for sulfur insertion in eukaryotic XO family enzymes. In prokaryotic XO and DMSOR families enzymes, two individual proteins, a desulfurase and a specific chaperon, interact to achieve sulfur insertion through a functionally similar mechanism.

XO family enzymes, sulfuration is catalyzed by a homodimeric two-domain molybdenum sulfurase, whose *N*-terminal domain shares structural and functional homologies to bacterial L-cysteine desulfurases IscS (in humans, the human molybdenum cofactor sulfurase (HMCS) was identified; ABA3 was identified in *Arabidopsis thaliana*) [111–113]. Their *N*-terminal IscS-type domain abstracts the cysteine sulfur to form a persulfide-sulfur in a conserved cysteine residue (Cys_{430} in ABA3), in a PLP-dependent reaction (Fig. 4, bottom) [114]. Subsequently, that sulfur is directly transferred to the molybdenum cofactor that is bound on the *C*-terminal domain of the molybdenum sulfurase (direct sulfur-transfer reaction) [111–118]. The now sulfurated molybdenum cofactor can then be incorporated into the enzyme. In prokaryotic XO family enzymes, a chaperon protein binds the molybdenum cofactor (*Rhodobacter capsulatus* XdhC is one of the best characterized ones); the chaperon then interacts with an L-cysteine desulfurase (*R. capsulatus* NifS4 [119]), which is responsible for the molybdenum sulfuration in a reaction similar to the one described above (abstraction of the cysteine sulfur and transient formation of a persulfide); after molybdenum sulfuration, the desulfurase dissociates and the chaperon with the now sulfurated center bound inserts it into the enzyme [110,119–125]. The sulfuration of DMSOR family enzymes that harbor a terminal sulfido group is also dependent on specific chaperon proteins [126–128] and IscS desulfurases [126,128,129]. In *E. coli*, the chaperon responsible for FDH maturation, FdhD, was shown to interact with an IscS and its Cys_{121} residue was suggested to be responsible for intermediating the sulfur transfer from IscS to the molybdenum, with its Cys_{124} promoting the release of the Cys_{121}-bound sulfide for subsequent catalysis [126]. Yet, the sulfur transfer mechanism in DMSOR family enzymes is still not well understood. This is further complicated by some FdhD homologues that do not have the corresponding Cys_{121} and Cys_{124} conserved, or do not need those residues to synthesize an active FDH, as is the case of the *R. capsulatus* homologue (FdsC) [49,127,130].

Overall, the molybdenum sulfuration depends on a cysteine desulfurase to provide sulfur and on a module to anchor the molybdenum cofactor. Eukaryotes evolved a single protein to carry out both functions. Prokaryotes use two individual proteins, where the specificity for the target enzyme is introduced by the chaperon protein; the cysteine desulfurase is used non-specifically for the sulfuration of a variety of sulfur-containing molecules, including the dithiolene moiety of PDT, as well as, the examples discussed above and many others.

5. Sulfide as catalyst: hydrogen atom transfer reactions

The metal-bound terminal sulfido present in some molybdo- and tungstoenzymes is crucial for the respective hydrogen atom transfer activity. The hallmark of this sulfide catalytic role is provided by the enzyme inhibition upon cyanide treatment, with release of thiocyanate, and subsequent activity restoration by incubation under reducing conditions with an exogenous sulfide source (usually Na_2S). The hydrogen atom transfer mechanism of two metal-bound sulfido-containing enzymes, XO and FDH, has been thoroughly probed by kinetic, spectroscopic, and structural methodologies and is presently well established. The current extraordinarily detailed picture of FDH and XO catalysis will be described in the next two sections.

5.1. Formate dehydrogenase catalysis

FDH are a heterogeneous and broadly distributed group of enzymes that catalyze the reversible two-electron interconversion of formate and CO_2 (Eq. 1) [18,19,49–51,131,132]. Prokaryotes use these enzymes to fix (reduce) CO_2 into formate, but also to derive energy, by coupling the formate oxidation to the reduction of several terminal electron acceptors; FDH are also broadly exploited in C1 metabolism by both prokaryotes and eukaryotes.

$$CO_2 + (2e- + H^+) \rightleftharpoons HCOO^- \quad (1)$$

There are two major classes of FDH: the metal-independent FDH (not relevant in the context of this review) [133–140] and the molybdenum and tungsten-dependent FDH (Mo-FDH and W-FDH) [141–178]. Noteworthy, besides the molybdenum or tungsten center, FDH also harbor other redox-active centers, involved in intramolecular and intermolecular electron transfer, such as Fe/S centers, hemes and flavins, organized in different subunit compositions and quaternary structures [18,19,49–51,131,132]. Despite this diversity, the active site of Mo-FDH and W-FDH is very well conserved and also similar to the one of molybdenum- and tungsten-containing *N*-formyl-methanofuran dehydrogenases (FMFDH), enzymes that catalyze the reduction of CO_2 to formate as well [179–182]. In the oxidized form, the active site of FDH and FMFDH enzymes harbors one molybdenum or tungsten ion coordinated by the *cis*-dithiolene (–S–C=C–S–) group of two pyranopterin cofactor molecules (Fig. 5 A) [18,19,49–51,131,132]. The metal first coordination sphere is completed by one terminal sulfido group (Mo^{6+}/W^{6+} = S) plus one sulfur or selenium atom from a cysteine or selenocysteine residue (Mo^{6+}/W^{6+}-S(Cys) or Mo^{6+}/W^{6+}-Se(SeCys)) (abbreviated as Cys-Mo-FDH, Cys-W-FDH, SeCys-Mo-FDH and SeCys-W-FDH), in a distorted trigonal prismatic geometry. Noteworthy, there is no apparent relation (as far as is presently known) between the metal and the bound amino acid residue or the enzyme activity (with Cys-Mo-FDH, Cys-W-FDH, SeCys-Mo-FDH and SeCys-W-FDH being known for many years). The active site also comprises two other residues that are strictly conserved to all known FDH and FMFDH and are thought to be crucial to the catalytic cycle, one arginine and one histidine.

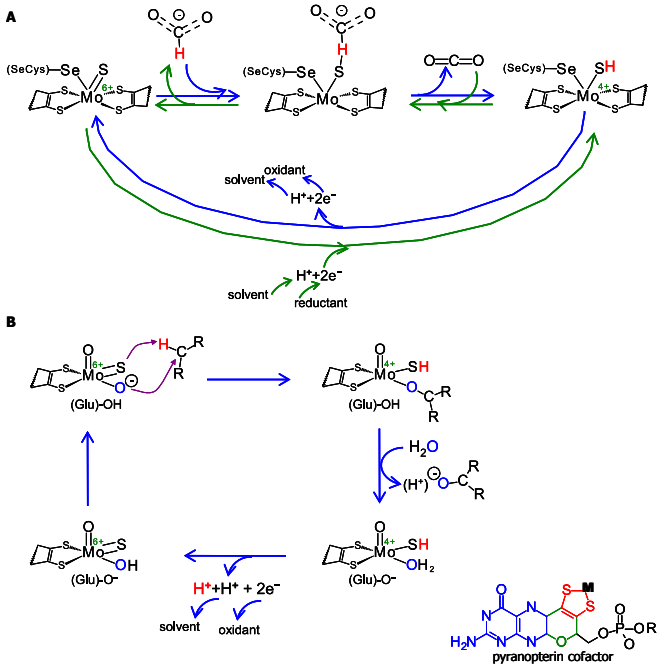

Fig. 5. Proposed reaction mechanism of (A) FDH and (B) XO. (A) Reversible mechanism of molybdenum- and tungsten-dependent FDH and FMFDH-catalyzed formate oxidation (blue arrows) and CO_2 reduction (green arrows), as proposed by [183,184]. A similar hydride transfer mechanism can also take place with a penta-coordinated reduced metal centre, with a dissociated selenocysteine/cysteine residue. For simplicity, the mechanism is represented only for a molybdenum, selenocysteine-containing enzyme, but it should be similar for tungsten and cysteine-containing enzymes. See text for details. In (B), R_2C-H and R_2C-O^- represent xanthine and urate moieties, respectively. In both (A) and (B), for simplicity, only the dithiolene moiety of the pyranopterin cofactor is represented. Bottom right: The complete structure of the molybdenum cofactor, pyrano(green)-pterin(blue)-dithiolene(red)-methylphosphate(black) is shown at the bottom; M stands for metal, Mo or W. All so far characterized FDH and FMFDH active sites harbor two cofactor molecules, both with the R position esterified with a guanosine monophosphate nucleotide (Mo/*W-bis*-PGD); the eukaryotic XO active site holds one non-sterified cofactor molecule (R = H; Mo-PMN), while in the prokaryotic XO active site R is esterifed with a cytidine monophosphate nucleotide (Mo-PCD). (For interpretation of the references to colour in this figure legend, the reader is referred to the web version of this article.)

In spite of the overall structural and metal/amino acid active site diversity, the reaction mechanism of CO_2/formate interconversion is accepted to be similar in all (so far known) FDH and FMFDH enzymes. For simplicity, the reaction mechanism will be herein illustrated with a Mo-SeCys-FDH.

As originally proposed by Niks et al. [183] for formate oxidation and shortly after also for CO_2 reduction by Maia et al. [184], CO_2/formate interconversion is presently recognized to occur through hydride transfer, with the sulfido group playing the central role of direct hydride acceptor and donor, Mo^{6+} = S and Mo^{4+}-SH, respectively (follow the red hydrogen atoms in Fig. 5 A). This behavior, metal oxidized/hydride acceptor versus metal reduced/hydride donor (eq. 2), is supported by a remarkable characteristic of the Mo/W-ligands: the pK_a values of the coordinated ligands change dramatically with the oxidation state of the metal and determine that the higher oxidation states should hold deprotonated ligands, that is Mo/W^{6+} = S, while the lower oxidation states should hold protonated ligands, that is Mo/W^{4+}-SH [185–187]. This feature enables the metal-sulfido to act as a hydride acceptor/donor [14,185–187,271].

$$Mo/W^{6+} = S + (2e- + H^+) \rightleftharpoons Mo/W^{4+}\text{-SH} \quad (2)$$

In accordance, formate oxidation (Fig. 5 A, blue arrows) is initiated with formate binding to the oxidized active site, but not directly to the molybdenum ion; instead, the conserved active site arginine residue is proposed to be essential to anchor the formate molecule with its Cα hydrogen pointing towards the sulfido ligand, through hydrogen bond (s) with its oxygen atom(s) [183,184]. Formate oxidation, then, proceeds by straightforward hydride transfer from formate to the sulfido group of the oxidized molybdenum centre, Mo^{6+} = S, leading to the formation of Mo^{4+}-SH and CO_2. The re-oxidation of Mo^{4+} to Mo^{6+} (via intramolecular electron transfer to the enzyme other(s) redox-active centre(s) and, eventually, to the physiological partner) and the release of CO_2 close the catalytic cycle. The pK_a of the terminal sulfido group dictates that the now oxidized Mo^{6+} should favor its deprotonation and the initial oxidized molybdenum centre, Mo^{6+} = S, is regenerated.

CO_2 reduction is suggested to follow the reverse reaction mechanism (Fig. 5 A, green arrows) [184,188–190]. CO_2 binds to the reduced active site, at the same site as formate, with the conserved arginine anchoring its oxygen atom(s) through hydrogen bond(s) and orienting its carbon atom towards the protonated sulfido ligand. Then, the reaction proceeds through straightforward hydride transfer from the protonated sulfido group of the reduced molybdenum centre, Mo^{4+}-SH, to the CO_2 carbon, whose LUMO has predominant C- π orbital character, prone to nucleophile attack and reduction. This yields a formate moiety and Mo^{6+} = S. The subsequent re-reduction of Mo^{6+} to Mo^{4+} (via intramolecular electron transfer from the enzyme physiological partner, through its redox centre(s)) and formate release close the catalytic cycle. The now reduced Mo/W^{4+} favors the sulfido group protonation and the initial reduced centre, Mo^{4+}-SH, is regenerated.

It should be noted that, presently, there is no consensus if the selenocysteine/cysteine residue remains bound to the metal in the reduced state, during catalysis (as discussed in [19]). Yet, although the mechanism is suggested to operate with a permanent hexacoordinated metal centre, it can also occur in a penta-coordinated centre (with an unbound selenocysteine/cysteine), since the sixth ligand should not interfere with the hydride transfer.

Overall, the FDH/FMFDH reaction is reversible and the equilibrium between formate oxidation versus CO_2 reduction is determined by the availability of formate versus CO_2 and the ability to maintain the active site oxidized versus reduced. The key feature responsible for the catalysis of this reversible reaction is the metal-bound terminal sulfido,

whose protonation state is determined in a concerted and straightforward way by the enzyme active site oxidation state.

5.2. Xanthine oxidase catalysis

XO is responsible for the hydroxylation of hypoxanthine and xanthine to urate (eq. 3) in almost all forms of Life [14,15,46,191–194] (only a small number of organisms (some yeasts [195]) use different enzymes to catabolize these purines [196–198]). Besides xenobiotic metabolism (due to its broad substrate specificity), XO is also involved in the generation of signaling nitric oxide generation [199–211], reactive oxygen species and in a multitude of oxidative stress-mediated pathological conditions [212–258].

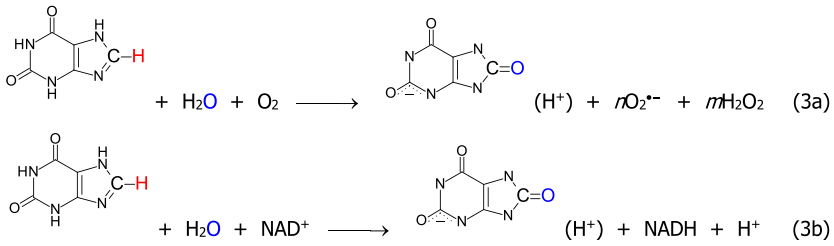

As in many other molybdoenzymes, besides the molybdenum center, mammalian XO also harbors other redox-active centers, in this case two [2Fe-2S] centers and one FAD, which are involved in intramolecular electron transfer to the physiological partner, molecular oxygen (XO form; eq. 3a) or NAD^+ (xanthine dehydrogenase form; eq. 3b) [259–265]. In the oxidized form, the XO active site harbors one molybdenum ion coordinated by the *cis*-dithiolene (–S–C=C–S–) group of one pyranopterin cofactor molecule, plus one axial oxido group, an equatorial catalytically labile Mo^{6+}-OH group and one equatorial terminal sulfido group (Mo^{6+} = S), in a square-pyramidal geometry (Fig. 2 A, Fig. 5 B). The XO active site comprises also a conserved glutamate residue, key to catalysis (Glu_{1261} in bovine XO).

As is characteristic of most molybdoenzymes, XO catalyzes an oxygen atom transfer reaction, transferring one oxygen atom from water to the substrate (follow the blue oxygen atoms in eq. 3 and Fig. 5 B) [14,15,46,191,192,194,259,261,266–271]. Yet, to accomplish the xanthine hydroxylation, a C—H bond must be hydrolyzed and a hydrogen atom acceptor must be present (red hydrogen atoms in eq. 3 and Fig. 5 B). The metal-bound terminal sulfido group fulfills this role in a way similar to the one described above for formate oxidation.

XO-catalyzed hydroxylation (as well as other XO family members; Fig. 5 B) is initiated with the activation of the molybdenum catalytically labile hydroxyl group (Mo-OH) by the conserved deprotonated glutamate residue, to form a Mo^{6+}-O^- core (base-assisted catalysis) [14,15,46,191–194]. The subsequent nucleophilic attack of Mo^{6+}-O^- on the carbon atom to be hydroxylated, with the simultaneous hydride transfer from the substrate to the sulfido group (Mo^{6+} = S to Mo^{4+}–SH), results in the formation of a covalent intermediate, Mo^{4+}-O-C-R(-SH) (where R represents the remainder of the substrate molecule). Hydrolysis of the Mo—O bond releases the hydroxylated product and yields a Mo^{4+}-$OH_{(2)}$(-SH) core. The re-oxidation of Mo^{4+} to Mo^{6+} (via intramolecular electron transfer, through the [2Fe—2S] and FAD, to molecular oxygen or NAD^+) closes the catalytic cycle. The pK_a of the terminal sulfido group dictates that the now oxidized Mo^{6+} should favor its deprotonation and the initial oxidized molybdenum centre, Mo^{6+} = S, is regenerated in a process similar to the one described for FDH/FMFDH.

Overall, water is the ultimate source of the oxygen atom incorporated into the hydroxylated product, as is characteristic of many molybdoenzymes: the molybdenum labile hydroxyl group (Mo-OH) that ends up in the reaction product (urate) is regenerated from a solvent water molecule when the catalytic cycle is closed (blue oxygen atoms in Fig. 5 B). The key catalytic role of hydride acceptor is performed by the metal-bound terminal sulfido, whose "correct" protonation state is ensured by the enzyme active site oxidation state.

6. Sulfide effects on catalysis

6.1. Sulfide effect on Ni,Fe-CODH catalysis

Ni,Fe-CODHs are found in anaerobic bacteria and archaea that catalyze the reversible oxidation of CO to CO_2 [7,272]. The crystal structures of the active site of Ni-Fe-CODH from *Carboxydothermus hydrogenoformans* ($CODH_{Ch}$), *Rhodospirillum rubrum* ($CODH_{Rr}$), and *Moorella thermoacetica* ($CODH_{Mt}$) have been reported [66,273–275]. The Ni-, Fe-, and S-containing active center is called cluster C. Interestingly, two types of active site structures are identified from these organisms. $CODH_{Ch}$ contains a bridged μ_2-sulfide ion that covalently connects the Ni and the distal Fe (forming a [Ni-4Fe-5S] center) (Fig. 6 A) [66], whereas $CODH_{Rr}$ and $CODH_{Mt}$ lack this bridge ([Ni-4Fe-4S]) (Fig. 6 B) [273]. Dobbek et al. reported a strong positive corelation between sulfide and enzyme activity, suggesting a catalitic role for the bridged μ_2-sulfide [276]. The inactivation of $CODH_{Ch}$ is caused by the loss of bridging sulfide from [Ni-4Fe-5S] leading to a [Ni-4Fe-4S] cluster upon long incubation of CO in $CODH_{Ch}$, that suggests that sulfide is required for catalytic activity [276]. On the other way, Feng and Lindahl [277] reported a different result, where oxidation of CO is prevented by incubation of sulfide in $[Ni\text{-}4Fe\text{-}4S]_{Rr}$ or $[Ni\text{-}4Fe\text{-}4S]_{Mt}$, proposing the formation of a [Ni-4Fe-5S] cluster. The activity can be restored by the reduction with CO and dithionite, because sulfide can not bind to the reduced state (Cred2) of $CODH_{Ch}$, and a sulfide bridging Ni and the distal Fe in Cred1 was proposed. So, the [Ni-4Fe-5S] cluster is an inactive site that is competent to bind CO [277]. A similar effect is observed upon addition of CN^- to Cred1 and it is released in the presence of reductant, suggesting a common mode of action like sulfide [278]. These data conclude that substrate H_2O can bind in the same mode of action like HS^- and CN^-. The crystal structure of reduced $CODH\text{-}II_{Ch}$ reveals that HO^- bridges Ni and distal Fe (Fig. 6 C) [279]. A proposed catalytic cycle of C-cluster in CODH is shown in Fig. 7, wherein C-cluster shows three redox states, namely, Cox, Cred1, and Cred2 [280]. Moreover, Wang et al. have reported that sulfide binds to the inactive Cox state of the C-cluster, inhibiting catalytic activity of CODH [281].

6.2. Sulfide effect on nitrogenase catalysis

Nitrogenase, a complex metalloprotein containing a heterometallic-cofactor, catalyzes the reduction of dinitrogen (N_2) to ammonium (NH_4^+) [9–11]. There are three types of nitrogenases, each harboring a different set of metals at its active site: the FeMoco, [Mo-7Fe-9S-C], the iron and vanadium-containing cofactor (FeVco), [V-7Fe-8S-C]) and the iron only-containing cofactor (Feco) [9–11] (Fig. 8). Unexpectedly,

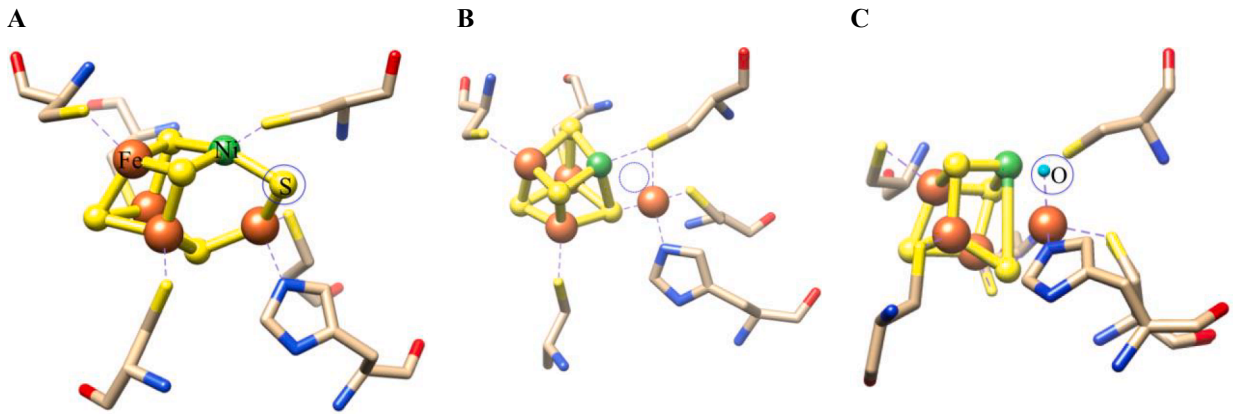

Fig. 6. Structures of (A) [Ni-3Fe-5S], (B) [Ni-3Fe-4S] and (C) [Ni-3Fe-4S-O]. In (B), the absent sulfide is indicated by the dotted blue circle. Structures shown are, respectively, from $CODH_{Ch}$ (PDB file 1SU6), $CODH_{Rr}$ (PDB file 1JQK) and $CODH\text{-}II_{Ch}$ (PDB file 3B53). (For interpretation of the references to colour in this figure legend, the reader is referred to the web version of this article.)

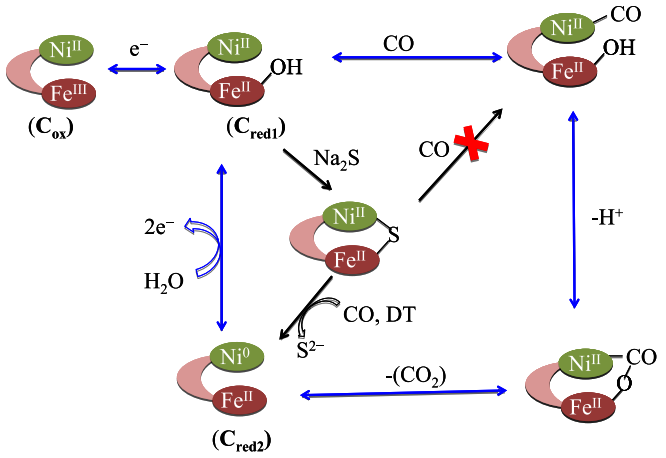

Fig. 7. Proposed catalytic mechanism of CODH and its reversible inhibition by sulfide. DT, dithionite.

FeVco lacks one bridged sulfide ion (S3A) compared to FeMoco, which is replaced by a bridging ligand, a μ_2-1,3-carbonate (Fig. 8 B). The well characterized resting state of MoFeco does not bind N_2, but it is believed that Fe2 and Fe6 are involved in the binding of N_2 [6]. In 2014, Rees et al. have reported a crystal structure of CO bound MoMo-co where CO binds at bridging sulfide (S2B) site of Fe2 and Fe6 by replacing it (Fig. 8 C) [282]. This is also supported by the CO binding VFeco, in which S2B dissociate from cluster Fe2-Fe6 upon binding of CO (Fig. 8 D) [65]. These results suggest that bridging S2B ligand is labile and dissociate reversibly during N_2 binding. In 2018, Sippel et al., have reported a crystal structure of N bound V-nitrogenase, in which S2B is protonated and dissociated from the V-Feco, but it is stored inside protein nearby Gln_{176} [65], indicating it can bind back easily to rebuild the cluster (Fig. 8 F). This result interprets that the S2B dissociates from the FeMo cluster upon N_2 binding. According to Lowe–Thorneley model, N_2 can bind to FeMoco until E4 state, designated as [Fe2–H–Fe6] (accumulation of 4e- and $4H^+$ on FeMo-cofactor) [283]. Recently, theoretical model of E4 state is designated as two hydrides bridging Fe2 and Fe6 with a terminal -SH group on either Fe2 or Fe6 [284] (Fig. 8 E).

6.3. Sulfide effect on the catalysis of particular nitrate reductases

Living organisms evolved different nitrate reductase (NaR) enzymes, all molybdenum-dependent, to reduce nitrate to nitrite [14,15,285]. Plants (and other eukaryotes) use an enzyme belonging to the sulfite oxidase family (eukNaR; Fig. 9 A) in the first and rate-limiting step of nitrate assimilation [286–292]. Prokaryotes are more versatile and use nitrate for assimilatory and dissimilatory processes and, for these purposes, these organisms hold three distinct NaR enzymes located in different subcellular spaces, all belonging to the DMSOR family [293–308]: (i) cytoplasmatic assimilatory NaR, involved in nitrogen assimilation (Fig. 9 B); (ii) respiratory NaR (Fig. 9 C), a membrane-bound cytoplasm-faced complex protein involved in the generation of a proton motive force across the cytoplasmatic membrane; (iii) periplasmatic NaR (Fig. 9 D and E) acting as an electron sink to eliminate excess of reducing equivalents or associated with the generation of a proton motive force.

To accomplish those diverse biological roles in different subcellular locations, these four enzymes have different subunit organizations and redox-active cofactor compositions, forming a group of heterogeneous proteins [14,15,285,303,304]. In addition, their molybdenum centers also present some subtle differences, as highlighted in Fig. 9 A to E. However, the feature that stands out in this group is the presence of a metal-bound terminal sulfido in some prokaryotic periplasmatic enzymes (*Cupriavidus necator* and *Desulfovibrio desulfuricans*) (Fig. 9 E).

Nitrate conversion into nitrite is a two-electron reduction, involving an oxygen atom abstraction reaction (follow the blue oxygen atoms in eq. 4).

$$ONO_2^- + 2e^- + 2H^+ \rightleftharpoons NO_2^- + H_2O$$

Several molybdoenzymes-catalyzed reactions involve the transfer of an oxygen atom from water to substrate (e.g., eq. 3) or from substrate to water (like this one, eq. 4), with the molybdenum ion cycling between the +6 and + 4 oxidation states [14,15]. Common to all these reactions is a molybdenum center with a free or labile coordination position (e.g., the XO equatorial labile Mo^{6+}-OH; Fig. 5 B). NaR enzymes, with a few exceptions (detailed below), follow this general mechanism. In eukNaR (Fig. 9 F) [286,287,309–313], catalysis is initiated with the enzyme reduction, to form a reduced molybdenum center with its equatorial labile oxido group protonated ($Mo^{6+} = O \rightarrow Mo^{4+}\text{-}OH_2$). Nitrate binding to the molybdenum, displacing the labile group, results in the formation of a covalent intermediate $Mo^{4+}\text{-}O\text{-}NO_2$. The subsequent O—N bond cleavage releases the product (nitrite) and regenerates the $Mo^{6+} = O$ core with a "fresh" labile oxido group.

A parallel mechanism is suggested to operate on prokaryotic enzymes, with their labile oxido group being converted into a water molecule, displaced and substituted by a nitrate molecule (Fig. 9G) [14,15,285,303,304,314,315]. Nitrite formation should proceed also in a similar way, regardless the nature of the amino acid bound to the metal (cysteine or aspartate) or the molybdenum center being di-oxo-pentacoordinated (Fig. 9 F) or mono-oxo-hexacoordinated (Fig. 9G).

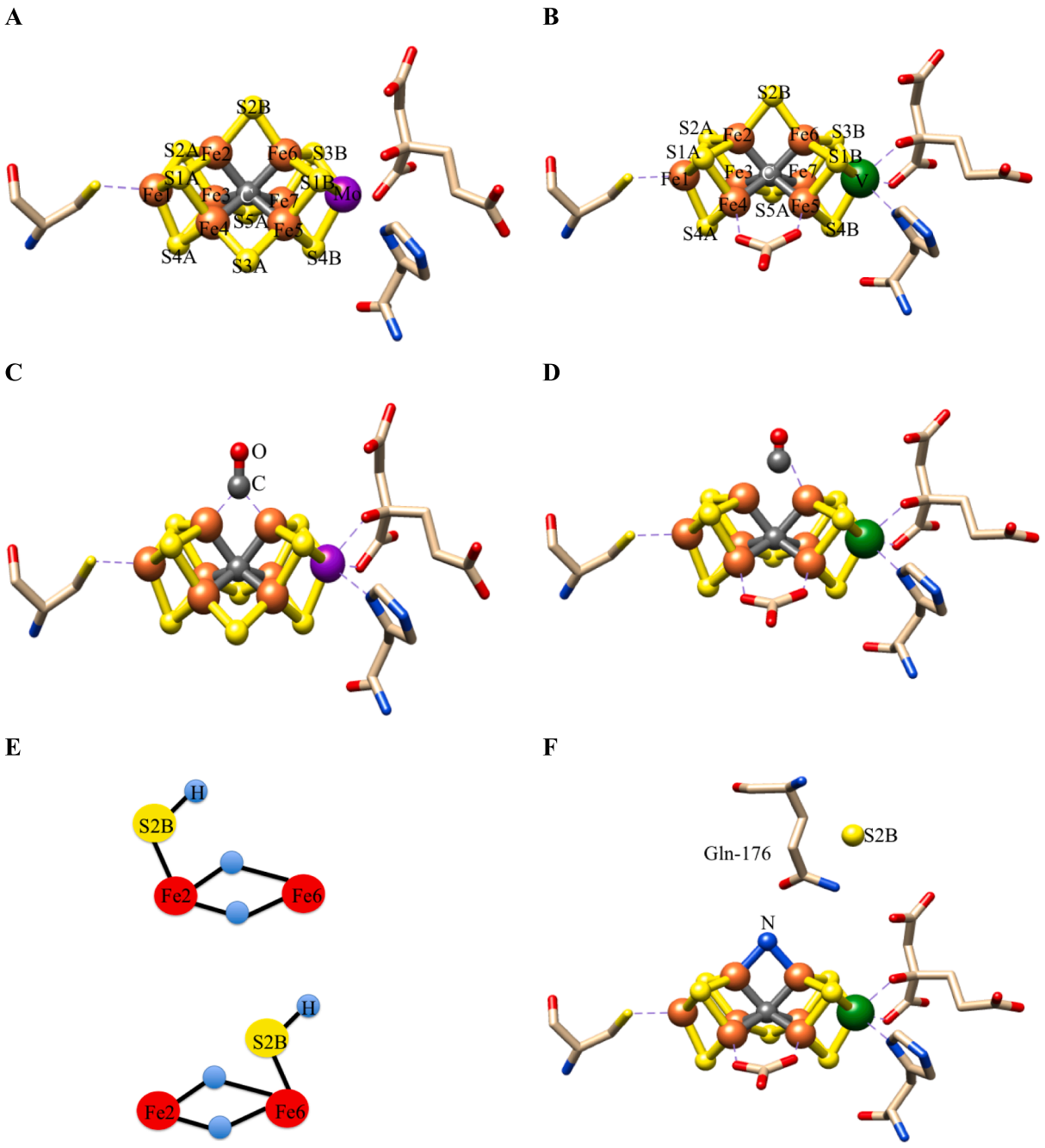

Fig. 8. Structure of (A) FeMoco [Mo-7Fe-9S-C], (B) FeVco, [V-7Fe-8S-C], (C) CO bound [Mo-7Fe-9S-C], (D) CO bound [V-7Fe-8S-C]. It is also represented (E) the proposed structure of the E4 state of FeMoco and (F) FeVco with a bound intermediate, interpreted as a μ_2-bridging, protonated nitrogen that implies the site and mode of substrate binding to the cofactor [65,284]. Structures shown are from *Azotobacter vinelandii* and based on PDB files 3U7Q (A), 5N6Y (B), 4TKV (C), 7ADR (D) and 6FEA (F).

The active site of periplasmatic NaR from *D. desulfuricans* and *C. necator*, however, is described as holding a complete, six sulfur-based coordination, with a metal-bound terminal sulfido ligand (Fig. 9 E) [316–319]. Lacking a free coordination position or a labile ligand, these enzymes do not fulfill the "oxo-transfer criteria" necessary to catalyze oxygen atom transfer. To explain the observed enzymes nitrate reduction activity, a theoretical calculations-based proposal was introduced, in which the as-isolated inactive NaR is first activated by displacement of the coordinated cysteine residue to form persulfide with the terminal sulfido group, Mo-S-S(Cys) (Fig. 9 H) [320]. This structural alteration, named as "sulfur-shift", creates a vacant coordination position in the molybdenum center. Catalysis can, then, proceed with nitrate binding and eventual nitrite formation and release, leaving a mono-oxo-hexacoordinated center. Hence, after the initial activating sulfur-shifting to remove the terminal sulfido, nitrate reduction by these particular enzymes can proceed as described for the other homologue enzymes.

Although the physiological relevance of the two alternating molybdenum coordinations remains to be established, as well as, the confirmation of different catalytic intermediates, these two particular NaR enzymes (*D. desulfuricans* and *C. necator*) provide a further example of the sulfide effects on catalysis.

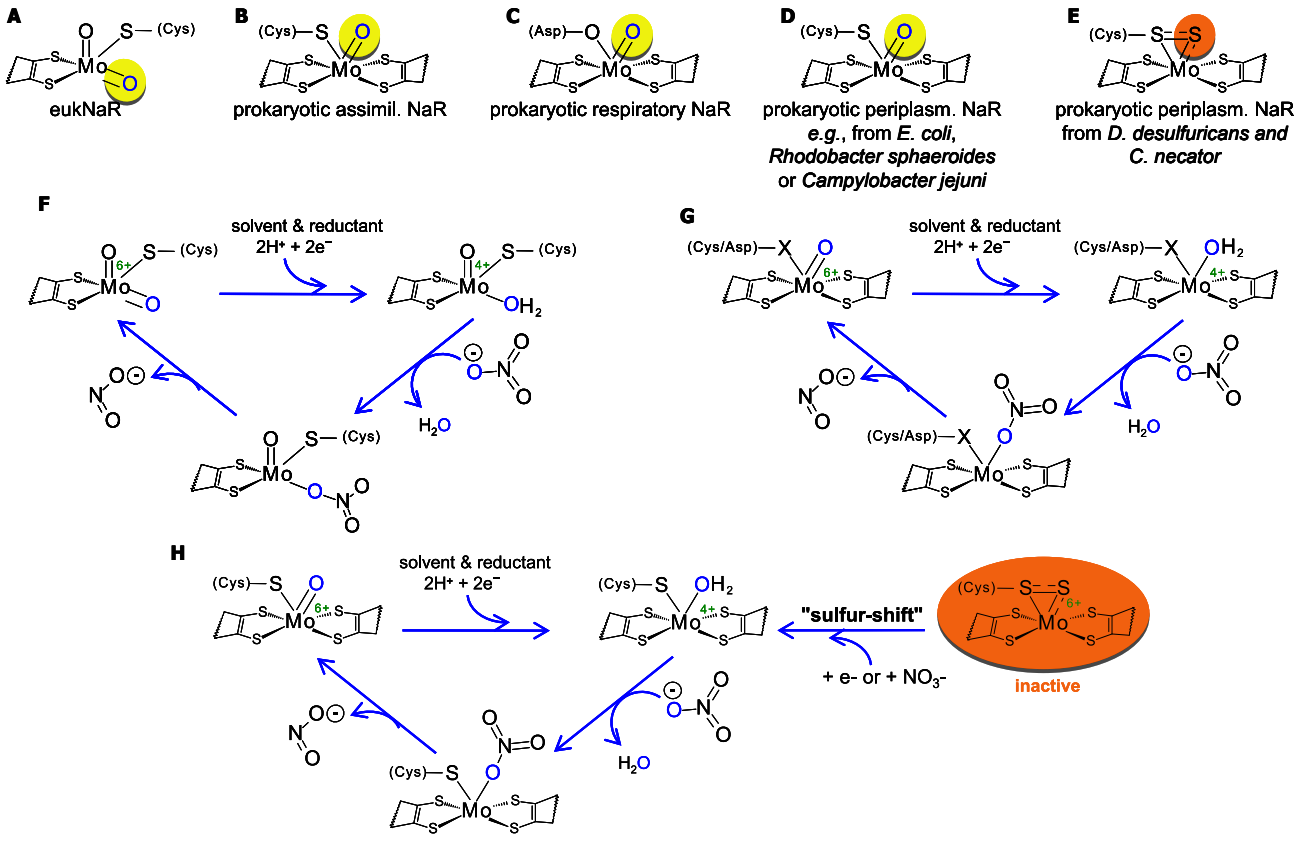

Fig. 9. (A) - (E) Active site molybdenum centers, in the oxidized state, of different nitrate reductase enzymes. (F), (G) Proposed reaction mechanism of eukNaR and prokaryotic NaR. (H) "Sulfur-shift" mechanism to activate prokaryotic periplasmatic from *D. desulfuricans* and *C. necator*. See text for details.

6.4. Protonation of sulfide in the redox process of 3Fe—4S cluster in proteins

Many active sites containing Fe/S clusters have pH-dependent reduction potential values, despite the variable protein environment, suggesting, in general, the protonation at the vicinity of cluster [321,322]. However, the redox potential of two most common clusters, [2Fe—2S] and [4Fe-4S], usually shows little dependence on pH, indicating no protonation involvement in the redox process [323]. By contrast, the redox chemistry of [3Fe-4S] clusters is strikingly different, with an intrinsic ability for protonation [324]. This protonation chemistry has been observed in all [3Fe—4S]-containing proteins, including the [3Fe—4S] ferredoxins from *Desulfovibrio gigas* (Fd II) [325], *Pyrococcus furiosus* [326], and beef heart aconitase [327], and [7Fe-8S] ([3Fe—4S] and [4Fe-4S]) ferredoxins from *Azotobacter Vinelandii* (Fd I) [328], *Desulfovibrio africanus* (Fd III) [329,330], and *Sulfolobus acidocaldarius* [324]. Interestingly, the structure of [3Fe-4S] cluster is an open-faced crown-like with three μ_2-S atoms that have effective sites for protonation [321]. This chemistry also indicates that [3Fe—4S] cluster shows Lewis basicity by coordinating a metal ion at open-faced, which is a flourished chemistry and found in many proteins, such as mitochondrial aconitase [331], *D. gigas* Fd II [325,332,333], *D. africanus* Fd III [330,334,335], *P. furiosus* Fd [336–338]. $[3Fe—4S]^{1+}$ cluster exhibit multiple electron-proton transfer agent, which can capture 1-, 2- and 3-e/H^+ to yield reduced $[3Fe\text{-}4S]^0$, $[3Fe—4S]^{1-}$, and $[3Fe\text{-}4S]^{2-}$ states respectively [324–328,339–341]. Three μ_2-S atoms at the "vacant corner" of the [3Fe—4S] cluster can capture H^+, possibility 3-H^+ forming a bond with three μ_2-S atoms [321].

6.5. Transportation of sulfide in biotin synthase

Biotin (also known as vitamin B7), an essential micro-nutrient for all domains of life, is a key prosthetic group required for carboxylation, decarboxylation, gluconeogenesis, and amino acid metabolism [342,343]. This prosthetic group is synthesized only by microbes and plants, in a reaction catalyzed by biotin synthase (BioB). The BioB, an iron-sulfur enzyme, catalyzes the conversion of dethiobiotin (DTB) to biotin by insertion of a sulfur atom into the DTB in the final step of biotin biosynthesis (Fig. 10) [344,345]. BioB is a member of the radical S-adenosyl-L-methionine (SAM or AdoMet) superfamily [346–348], and

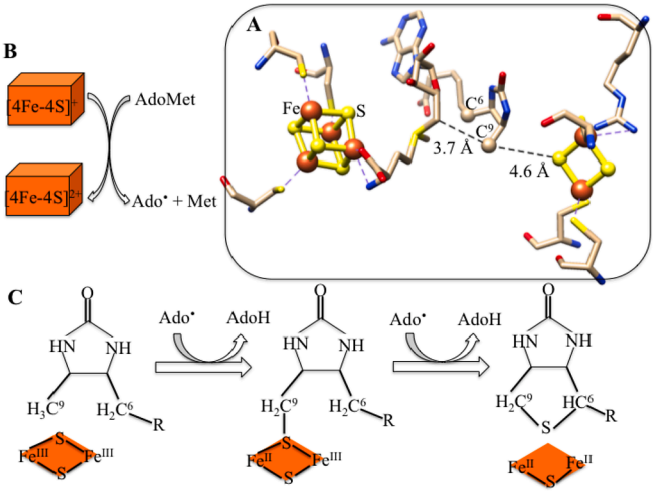

Fig. 10. (A) Structure of the biotin synthase active site containing AdoMet bound [4Fe-4S], dethiobiotine and [2Fe-2S] (PDB file 1R30). (B) [4Fe—4S] facilitates the formation of Ado• radical. (C) [2Fe—2S] cluster-derived sulfur atom insertion into dethiobiotin. Modified from [345].

its active site is composed of two Fe/S clusters - SAM binding [4Fe—4S] cluster, and an auxiliary [2Fe-2S] cluster, each with a key role in catalysis [347,349–352]. SAM-[4Fe—4S] cluster promotes reductive cleavage of the sulfonium C—S bond of SAM to generate a 5-deoxyadenosyl radical (5-dAdo), which abstracts hydrogen atoms from the C^9 methyl group of DTB, resulting in the formation of a dethiobiotinyl methylene carbon radical [353], which is finally quenched by a sulfur atom and yields biotin. Interestingly, this sulfur source is not from PLP-dependent cysteine desulfurase, rather from auxiliary $[2Fe\text{-}2S]^{2+}$ cluster wherein μ_2-S is a true sulfur source. The $[2Fe—2S]^{2+}$ cluster is close to DTB (~4.6 Å) (Fig. 10 A), suggesting transportation of μ_2-S to DTB (Fig. 10) [345,354]. So, in biothin synthesis, $[4Fe—4S]^{2+}$ cluster involves in electron transfer to SAM, while the $[2Fe—2S]^{2+}$ cluster involves in the sulfur insertion in DTB. During a single turnover of catalysis, a combined UV/visible and EPR results concludes that $[4Fe—4S]^{2+}$ cluster is conserved, while the auxiliary $[2Fe\text{-}2S]^{2+}$ cluster is lost, indicating oxidative loss of sulfur atom [345,355]. In addition, EPR spectroscopic studies identified an intermediate species that linked between [2Fe–2S] cluster and DTB through C—S bond [354].

7. Sulfide as substrate: heme and zinc-containing enzymes

Sulfide is formed endogenously, by desulfuration of amino acids (cysteine, and methionine), acid dissociation of Fe/S clusters in proteins (acid labile sulfide), or reduction of polysulfides. Cysteine desulfuration is achieved by three distinct enzymes, cystathionine β-synthase (CBS), γ-cystathionase (CSE), and mercaptopyruvate sulfurtransferase (MST) [356–359]. Prokaryotes such as the purple and green sulfur bacteria live in sulfide rich environments by extracting energy from the oxidation of sulfide, which however is a potent toxin for other organism at elevated concentration [365–359]. Therefore, cellular H_2S in humans is detoxified by canonical (mitochondria) [360] and non-canonical (red blood cell) sulfide oxidation pathways [361–365], by transforming it into thiosulfate and sulfate. However, sulfide acts as an inhibitor of cytochrome *c* oxidase (CcO) in mitochondria [1].

7.1. Cytochrome c oxidase

Mitochondrial cytochrome *c* oxidase (CcO) catalyzes the reduction of O_2 to H_2O in the final step of aereobic "respiration" [366–368]. The CcO comprises two heme iron centers (heme a and heme a_3), and two copper centers (CuA and CuB); the catalytic center of CcO consists of heme a_3, CuB, and a tyrosine residue. H_2S is generated in mitrochondria, and induces the modification of heme and Cu centers, inhibiting the enzyme activity reversibly [369–370]. In 1929, Keilin first observed that the activity of CcO was reduced by H_2S gas [371]. After that, Nicholls and others reported that H_2S inhibits CcO activity and also acts as a substrate/electron donor depending on H_2S concentration (Fig. 11) [372–375]. At low concentrations (stoichiometric ratio of CcO:H_2S = 1:1), H_2S binds and reduces the Fe^{III}-heme a_3 center to yield Fe^{II}-heme a_3-$^{\bullet}$SH intermediate, which further reacts with O_2 or another HS^- molecule to release $HOOS^{\bullet}$ or $H_2S_2^{\bullet}$, and Fe^{II}-heme a_3, suggesting that H_2S acts as a substrate rather than an inhibitor [375,376]. At moderate concentrations (CcO:H_2S = 1:2 stoichiometry), H_2S also binds and reduces the $Cu^{II}B$ center to yield a stable $Cu^{I}B$-SH complex. The Fe^{II}-heme a_3 may also reduce the $Cu^{II}B$ center to yield $Cu^{I}B$-Fe^{III}-heme a_3 complex, which binds HS^- to yield stable HS-$Cu^{I}B$-Fe^{III}-heme-a_3 intermediate. It is assumed that heme a_3-CuB-SH complex undergoes a conformational change, which may be unable to bind O_2. At higher H_2S concentrations (CcO:H_2S = 1:3 stoichiometry), both $Cu^{I}B$ and Fe^{III}-heme a_3 strongly bind HS^-, resulting full inhibition of CcO activity [1].

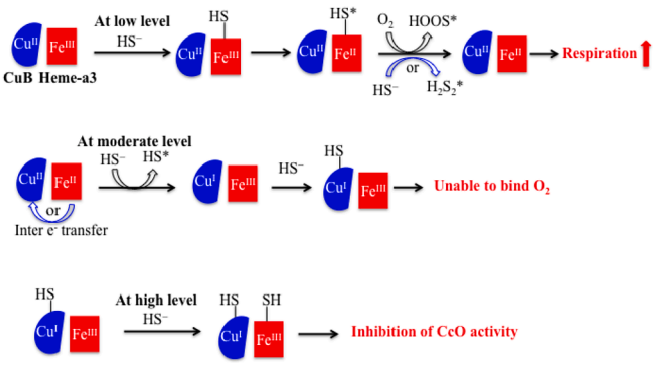

Fig. 11. Effect of different concentration of H_2S on CcO function. The figure is modified from [1].

7.2. Heme-proteins

In sulfide-rich environments, the interaction between sulfide and heme-proteins has a relevant role. Sulfide homeostasis, in humans, is facilitated by heme proteins, removing sulfide as thiosulfate and sulfate, through non-canonical sulfide oxidation pathways [32,356]. Red blood cells can synthesize H_2S, but cannot discard the toxic H_2S through the mitochondrial sulfide oxidation pathway due to the lack of mitochondria. Therefore, sulfide can bind to hemeproteins such as hemoglobin (Hb) and myoglobin (Mb) [377], undergoing two distinct chemical reactions: (1) sulfur atom incorporation in the pyrrole ring of heme, and (2) catalytic oxidation of sulfide [378,379]. In 1863, Hoppe-Seyler first observed that Hb-O_2 can react with H_2S to yield green product, suggesting the formation of sulfhemoglobin [380–382]. The sulfhemoglobin derivative is a covalent addition of sulfur to one of the heme pyrrole rings [383,384], but sulfide does not occupy the distal site of the heme iron. Michel et al. also showed that the analogous compound, sulfmyoglobin, is generated by the reaction of Mb-O_2 with H_2S [382,385]. The crystal structure of cyanomet-sulfmyoglobin C from horse heart has been reported and reveals that sulfur can covalently modify the pyrrole ring (Fig. 12 A) [383]. The sulfheme derivative has lower O_2 affinity [386], and increased levels of sulfhemoglobin cause a rare blood disease, sulfhemoglobinemia [387,388]. The proposed mechanism of sulfhemoglobin formation is that Hb (or Mb) interacts with H_2O_2 to yield ferryl Compound-I, (Fe^{IV}=O Por$^{\bullet+}$) and ferryl Compound-II (Fe^{IV}=O Por) [389], which may react with H_2S to produce the sulfheme derivative (Fig. 12 B) [390,391]. In addition, the distal His residue plays a key role in the formation of sulfheme formation. The intermediate His-ferryl-heme interacts with H_2S to yield a His-ferryl-heme ternary

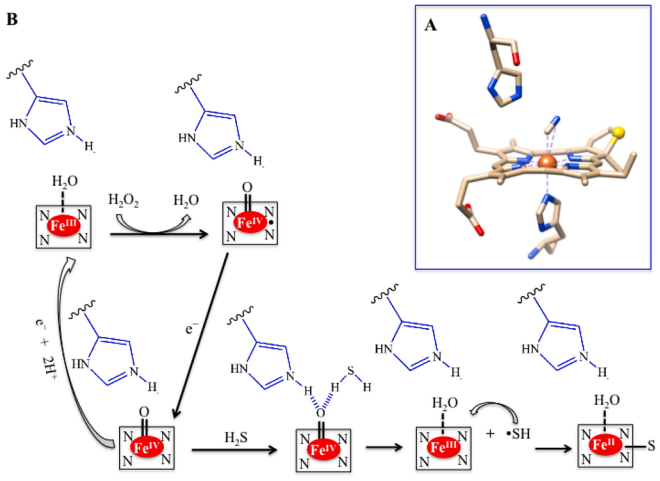

Fig. 12. (A) Structure of cyanomet-sulfmyoglobin and (B) proposed mechanism for the formation of sulfmyoglobin. Structure shown is from horse heart (PDB file 1YMC); S and Fe are represented by yellow and red spheres, respectively. (For interpretation of the references to colour in this figure legend, the reader is referred to the web version of this article.)

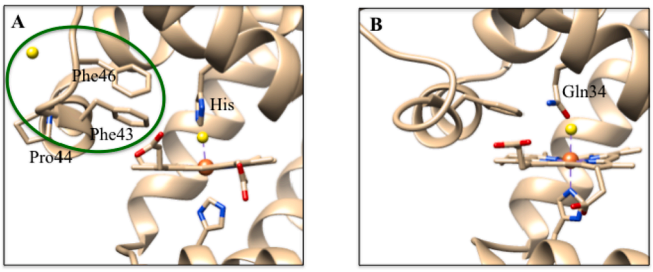

Fig. 13. Structure of sulfide adduct of (A) human myoglobin and (B) *Lucina pectinata* hemoglobin I. Structures shown are from PDB files 5UCU and 1MOH, respectively; S and Fe are represented by yellow and red spheres, respectively. (For interpretation of the references to colour in this figure legend, the reader is referred to the web version of this article.)

complex, which triggers the sulfheme formation [377,392]. Therefore, the formation of sulfheme at moderate levels and destruction of H_2S by red blood cells is considered a possible detoxification pathway of H_2S in humans [393].

However, other hemoglobins from other organisms that live in sulfide rich environments, such as clam *Lucina pectinata*, lack a distal His and this results in no formation of sulfheme as in human Hb/Mb [378,389]. This organism has three peculiar hemoglobins, with HbI binding and transporting H_2S, while HbII and HbIII are O_2 reactive proteins [378]. It is noticeable that in the presence of H_2O_2 and H_2S, HbI forms ferryl compound without formation of sulfheme [389]. The H_2S binds at the distal site and reduces heme-Fe^{III}-H_2S to heme-Fe^{II}-$HS^{\bullet}$ radical, which can further react with excess HS^- or O_2 to yield polysulfides or thiosulfate (Fig. 13). The crystal structure of sulfide bound Hb in *L. pectinata* has been reported (Fig. 13). The affinity of Hb1 for sulfide is higher compared to human Hb, due to the presence of a glutamine (Gln) residue at the distal site, over equivalent histidine (His) [394,395] (Fig. 13). *L. pectinata* HbI transports H_2S to symbiotic bacteria, which assimilate it and provide the host with a source of organic sulfur.

The binding of hydrogen sulfide to human Hb and Mb and formation of polysulfides or thiosulfate have been also reported, suggesting alternative pathways for detoxification of sulfide [365,396]. The crystal structure reveals that the sulfide ligand binds to the distal site of the heme iron. Interestingly, a second sulfide is located at the protein surface near the Phe/Pro path, and is proposed as an entry/exit channel for iron ligands/substrates (Fig. 13) [397]. The Hb-Fe^{III}-SH adduct may exchange the electron between Fe and S and exists in equilibrium with [Fe^{II}-$HS^{\bullet}$], which can react with another molecule of HS^- to yield $H_2S_2^{\bullet-}$. Coordinated $H_2S_2^-$ complex further reacts with HS^- and O_2 to yield the final compound thiosulfate (Fig. 14).

7.3. Zinc-containing enzymes

The interactions between H_2S and redox inactive Zn-proteins are relatively poorly studied compared to hemeproteins [1]. Zn-containing proteins, particularly the Zn-finger (ZF) motif, coordinated by His and Cys residues, play a key role in eukaryotic cells as transcription factors, which regulate gene transcription [398]. For instance, H_2S represses androgen receptor (AR) transactivation, by modulating the zinc-finger site [399]. AR contains two Zn-finger sites, which regulate the AR in the recognition of androgen-responsive elements [400], resulting in the development of prostate cancer [399]. In all catalytic Zn-sites in proteins, the Zn is coordinated to at least one H_2O molecule and three or four protein derived amino acid residues, a combination of histidine, cysteine, glutamate, and aspartate [401,402]. The Zn-bound H_2O molecule is a key component for catalysis because it can be either ionized (as in carbonic anhydrase) or polarized (as in carboxypeptidase

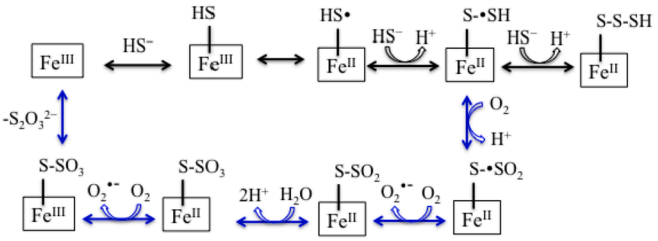

Fig. 14. Proposed mechanism for the conversion of H_2S to thiosulfate and heme iron-bound polysulfides by Hb. This is modified from [365].

A) by a base, or displaced by the substrate (as in alkaline phosphatase) [403,404]. In a similar way to the direct interaction with heme iron in heme-proteins, H_2S can also bind directly to the Zn-site by replacing the Zn-bound H_2O molecule, inhibiting the enzyme activity, as is observed in the angiotensin-converting enzyme [405]. Furthermore, H_2S may also interact with thiols in proteins to yield perthiols [406]. The thiol-to-perthiol conversion can significantly change the enzyme's function, as illustrated by the post-translational modification of the androgen receptor active site cysteine residue (Zn-Cys) upon S-sulfhydration by H_2S [407]. One proposed mechanism suggests that H_2S does not directly coordinate to the Zn center but facilitates S-sulfhydration at the Zn-Cys site in the Zn-finger [399,408]. Although Zn is redox inactive, it is thought to facilitate the S-sulfhydration by lowering the redox potential of Cys. In addition, phosphodiesterase 5 is a Zn^{II}-enzyme, which is inhibited by nanomolar concentrations of H_2S [409]. So, Zn^{II}-enzymes play a catalytic role in biology and might be inhibited by H_2S, such as angiotensin converting enzyme (ACE), carbonic anhydrase, and matrix protein [410,411]. It has been recently reported that H_2S may halt SARS-CoV-2 entry into the host cells by interfering with angiotensin converting enzyme 2 (ACE2) [412]. H_2S also regulates the function of metallothioneins (MTs), which are Cys-rich proteins that bind the Zn^{II} ion and detoxify heavy metals [413]. It has been noticed that H_2S inhibits Cd^{II} mediated toxicity by stabilizing the Zn-MT-1 isoform [414]. Zn-proteins may also transport H_2S. Indeed, a sulfide-adapted organism, tubeworm *Riftia pachyptila*, lives in a symbiotic relationship with sulfide-oxidizing bacteria, which use a uncommon Zn^{II}-containing hemoglobin to capture and transport H_2S through the bloodstream [415,416].

8. Summary and outlook

Sulfur has been shown to be a versatile ligand towards transition metals. The wide range of coordination modes leads to different architectures from mononuclear to polynuclear (homo and hetero) metal-sulfur clusters due to the variety of binding modes, including terminal μ_2-S, μ_3-S and μ_4-S. In addition, the different protonation and redox states that can be attained increase the dimension of possibilities. In a biological medium, the traditional insoluble metal sulfides are incorporated in a quasi-spontaneous self-assembly process, and both simple and complex clusters, invoking sulfur and metals, are organized. The chemistry is so fascinating that an assembly of simple and complex clusters can be obtain in vivo and in vitro, and the structures are so versatile that rearrangements and interconversions (addition and removal of metals) can occur to yield an extraordinary insight for cluster assembly and a meaning for the biological roles where they are engaged. The aim of this mini review is to highlight the description of structures containing sulfur and transition metals that have been described in the literature. Emphasis is given to the variety of clusters that can occur, and the role of sulfur in catalysis. Sulfur is far from being an "innocent ligand", and it actively participates in atom transfer and as a regulator/inhibitor of biochemical processes that may occur in high concentrations of H_2S.

Declaration of Competing Interest

The authors declare that they have no known competing financial interests or personal relationships that could have appeared to influence the work reported in this paper.

Acknowledgements

BKM thanks to NIT-Sikkim. LBM thanks Fundação para a Ciência e a Tecnologia, MCTES (FCT/MCTES), for the CEEC-Individual 2017 Program Contract. JJGM and LBM also received financial support from PT national funds (FCT/MCTES) through projects PTDC/BTA-BTA/0935/2020, UIDB/50006/2020 and UIDP/50006/2020.

References

[1] M.R. Filipovic, J. Zivanovic, B. Alvarez, R. Banerjee, Chemical biology of H2S signaling through persulfidation, Chem. Rev. 118 (2018) 1253–1337.
[2] E.I. Stiefel, In transition metal sulfur chemistry, in: E.I. Stiefel, K. Matsumoto (Eds.), ACS Symposium Series vol. Chapter 1, American Chemical Society, Washington, DC, 1996, pp. 2–38.
[3] M.K. Johnson, Iron-sulfur proteins: new roles for old clusters, Curr. Opin. Chem. Biol. 2 (1998) 173–181.
[4] H. Beinert, A tribute to sulfur, Eur. J. Biochem. 267 (2000) 5657–5664.
[5] D. Kessler, Enzymatic activation of sulfur for incorporation into biomolecules in prokaryotes, FEMS Microbiol. Rev. 30 (2006) 825–840.
[6] B.M. Hoffman, D. Lukoyanov, Z.-Y. Yang, D.R. Dean, L.C. Seefeldt, Mechanism of nitrogen fixation by nitrogenase: the next stage, Chem. Rev. 114 (2014) 4041–4062.
[7] M. Can, F.A. Armstrong, S.W. Ragsdale, Structure, function, and mechanism of the nickel metalloenzymes, CO dehydrogenase, and acetyl-CoA synthase, Chem. Rev. 114 (2014) 4149–4174.
[8] J. Liu, S. Chakraborty, P. Hosseinzadeh, Y. Yu, S. Tian, I. Petrik, A. Bhagi, Y. Lu, Metalloproteins containing cytochrome, iron–sulfur, or copper redox centers, Chem. Rev. 114 (2014) 4366–4469.
[9] O. Einsle, D.C. Rees, Structural enzymology of nitrogenase enzymes, Chem. Rev. 120 (2020) 4969–5004.
[10] L.C. Seefeldt, Z.-Y. Yang, D.A. Lukoyanov, D.F. Harris, D.R. Dean, S. Raugei, B. M. Hoffman, Reduction of substrates by nitrogenases, Chem. Rev. 120 (2020) 5082–5106.
[11] H.L. Rutledge, F.A. Tezcan, Electron transfer in nitrogenase, Chem. Rev. 120 (2020) 5158–5193.
[12] S.R. Pauleta, C. Carreira, I. Moura, Insights into nitrous oxide reductase, metalloenzymes in denitrification: applications and environmental impacts, RSC Metallobiol. 9 (2017) 141–169.
[13] S.R. Pauleta, M.S. Carepo, I. Moura, The treta copper-sulfide center of nitrous oxide reductase, in: Transition Metals and Sulfur- a Strong Relationship with Life, Berlin, p.Chapter 5, 2019.
[14] R. Hille, J. Hall, P. Basu, The mononuclear molybdenum enzymes, Chem. Rev. 114 (2014) 3963–4038.
[15] L.B. Maia, I. Moura, J.J.G. Moura, Molybdenum and tungsten-containing enzymes - An overview, in: R. Hille, C. Schulzke, M.L. Kirk (Eds.), Molybdenum and Tungsten Enzymes: Biochemistry, RSC Metallobiology Series No. 5 Chap 1, The Royal Society of Chemistry, Cambridge, 2017, pp. 1–80.
[16] R. Breglia, F. Arrigoni, M. Sensi, C. Greco, P. Fantucci, L.D. Gioia, M. Bruschi, First-principles calculations on Ni,Fe-containing carbon monoxide dehydrogenases reveal key stereoelectronic features for binding and release of CO2 to/from the C-cluster, Inorg. Chem. 60 (2021) 387–402.
[17] U. Terranova, Residues surrounding the active Centre of carbon monoxide dehydrogenase are key in converting x to CO, J. Biol. Inorg. Chem. (2021), https://doi.org/10.1007/s00775-021-01878-4.
[18] D. Niks, R. Hille, Molybdenum- and tungsten-containing formate dehydrogenases and formylmethanofuran dehydrogenases: structure, mechanism, and cofactor insertion, Protein Sci. 28 (2019) 111–122.
[19] L.B. Maia, I. Moura, J.J.G. Moura, Carbon dioxide utilisation - the formate route, in: J.J.G. Moura, I. Moura, L.B. Maia (Eds.), Enzymes for Solving Humankind's Problems Chap 2, Springer, Cham, 2021, pp. 29–81.
[20] G.N. George, I.J. Pickering, E.Y. Yu, R.C. Prince, S.A. Bursakov, O.Y. Gavel, I. Moura, J.J.G. Moura, A novel protein-bound copper−molybdenum cluster, J. Am. Chem. Soc. 122 (2000) 8321–8322.
[21] B.K. Maiti, L.B. Maia, S.R. Pauleta, I. Moura, J.J.G. Moura, Protein-assisted formation of molybdenum heterometallic clusters: evidence for the formation of S2MoS2–M–S2MoS2 clusters with M = Fe, co, Ni, cu, or cd within the orange protein, Inorg. Chem. 56 (2017) 2210–2222.
[22] J.J.G. Moura, A.L. Macedo, P.N. Palma, Ferredoxins, Methods Enzymol. 243 (1994) 165–188.
[23] D.C. Johnson, D.R. Dean, A.D. Smith, M.K. Johnson, Structure, function, and formation of biological iron-sulfur clusters, Annu. Rev. Biochem. 74 (2005) 247–281.
[24] B.K. Maiti, I. Moura, J.J.G. Moura, S.R. Pauleta, The small iron-sulfur protein from the ORP operon binds a [2Fe-2S] cluster, Biochim. Biophys. Acta 2016 (1857) 1422–1429.
[25] R.H. Holm, W. Lo, Structural conversions of synthetic and protein-bound iron–sulfur clusters, Chem. Rev. 116 (2016) 13685–13713.
[26] P. Zanello, The competition between chemistry and biology in assembling iron–sulfur derivatives. Molecular structures and electrochemistry. Part V. proteins, Coord. Chem. Rev. 335 (2017) 172–227.
[27] S.J. Cooper, C.D. Garner, W.R. Hagen, P.F. Lindley, S. Bailey, Hybrid-cluster protein (HCP) from Desulfovibrio vulgaris (Hildenborough) at 1.6 Å resolution†, Biochemistry 39 (2000) 15044–15054.
[28] D. Aragão, S. Macedo, E.P. Mitchell, C.V. Romão, M.Y. Liu, C. Frazão, L. M. Saraiva, A.V. Xavier, J. LeGall, W.M.A.M. van Dongen, W.R. Hagen, M. Teixeira, M.A. Carrondo, P. Lindley, Reduced hybrid cluster proteins (HCP) from Desulfovibrio desulfuricans ATCC 27774 and Desulfovibrio vulgaris (Hildenborough): X-ray structures at high resolution using synchrotron radiation, J. Biol. Inorg. Chem. 8 (2003) 540–548.
[29] T. Fujishiro, M. Ooi, K. Takaoka, Crystal structure of *Escherichia coli* class II hybrid cluster protein, HCP, reveals a [4Fe-4S] cluster at the N-terminal protrusion, FEBS J. 85 (2021), https://doi.org/10.1111/febs.16062.
[30] E. Cuevasanta, M.N. Möller, B. Alvarez, Biological chemistry of hydrogen sulfide and persulfides, Arch. Biochem. Biophys. 617 (2017) 9–25.
[31] M.N. Hughes, M.N. Centelles, K.P. Moore, Making and working with hydrogen sulfide: the chemistry and generation of hydrogen sulfide in vitro and its measurement in vivo: a review, free Radic, Biol. Med. 47 (2009) 1346–1353.
[32] Q. Li, J.R. Lancaster Jr., Chemical foundations of hydrogen sulfide biology, Nitric Oxide 35 (2013) 21–34.
[33] W.H. Koppenol, P.L. Bounds, Signaling by sulfur-containing molecules. Quantitative aspects, Arch. Biochem. Biophys. 617 (2017) 3–8.
[34] J. Rost, S. Rapoport, Reduction-potential of glutathione, Nature 201 (1964) 185.
[35] D. Voet, J.G. Voet, Introduction to metabolism, in: D. Harris, P. Fitzgerald (Eds.), Biochemistry, John Wiley & Sons, Inc, Hoboken, NJ, 2004, p. 573.
[36] T.V. Mishanina, M. Libiad, R. Banerjee, Biogenesis of reactive sulfur species for signaling by hydrogen sulfide oxidation pathways, Nat. Chem. Biol. 11 (2015) 457–464.
[37] T.N. Das, R.E. Huie, P. Neta, S. Padmaja, Reduction potential of the sulfhydryl radical: pulse radiolysis and laser flash photolysis studies of the formation and reactions of •SH and HSSH•- in aqueous solutions, J. Phys. Chem. A 103 (1999) 5221–5226.
[38] J.M. Fukuto, S.J. Carrington, D.J. Tantillo, J.G. Harrison, L.J. Ignarro, B. A. Freeman, A. Chen, D.A. Wink, Small molecule signaling agents: the integrated chemistry and biochemistry of nitrogen oxides, oxides of carbon, dioxygen, hydrogen sulfide, and their derived species, Chem. Res. Toxicol. 25 (2012) 769–793.
[39] S.W. Benson, Thermochemistry and kinetics of sulfur-containing molecules and radicals, Chem. Rev. 78 (1978) 23–35.
[40] D.C. Dittmer, Hydrogen Sulfide, Encyclopedia of Reagents for Organic Synthesis, Wiley, New York, 2010.
[41] A.K. SenGupta, Ion Exchange in Environmental Processes: Fundamentals, Applications and Sustainable Technology, John Wiley & Sons, Inc, New Jersey, USA, 2017.
[42] S.C. Lee, W. Lo, R.H. Holm, Developments in the biomimetic chemistry of cubane-type and higher nuclearity iron–sulfur clusters, Chem. Rev. 114 (2014) 3579–3600.
[43] I. Moura, J.J.G. Moura, E. Munck, V. Papaefthymiou, J. LeGall, Evidence for the formation of a cobalt-iron-sulfur (CoFe3S4) cluster in Desulfovibrio gigas ferredoxin II, J. Am. Chem. Soc. 108 (1986) 349–351.
[44] W.R. Hagen, Tungsten-containing enzymes, in: R. Hille, C. Schulzke, M.L. Kirk (Eds.), Molybdenum and Tungsten Enzymes: Biochemistry, RSC Metallobiology Series No. 5 vol. Chap 10, The Royal Society of Chemistry, Cambridge, 2017, pp. 313–342.
[45] R. Hille, The mononuclear molybdenum enzymes, Chem. Rev. 96 (1996) 2757–2816.
[46] T. Nishino, K. Okamoto, S. Leimkuhler, Enzymes of the xanthine oxidase family, in: R. Hille, C. Schulzke, M.L. Kirk (Eds.), Molybdenum and Tungsten Enzymes: Biochemistry, RSC Metallobiology Series No. 5 vol. Chap 6, The Royal Society of Chemistry, Cambridge, 2017, pp. 192–239.
[47] S. Grimaldi, B. Schoepp-Cothenet, P. Ceccaldi, B. Guigliarelli, A. Magalon, The prokaryotic Mo/W-bisPGD enzymes family: a catalytic workhorse in bioenergetic, Biochim. Biophys. Acta 1827 (2013) 1048–1085.
[48] A. Magalon, P. Ceccaldi, B. Schoepp-Cothenet, The prokaryotic Mo/W-bisPGD enzymes family, in: R. Hille, C. Schulzke, M.L. Kirk (Eds.), Molybdenum and Tungsten Enzymes: Biochemistry, RSC Metallobiology Series No. 5 vol. Chap 5, The Royal Society of Chemistry, Cambridge, 2017, pp. 143–191.
[49] T. Hartmann, N. Schwanhold, S. Leimkühler, Assembly and catalysis of molybdenum or tungsten-containing formate dehydrogenases from bacteria, Biochim. Biophys. Acta 2015 (1854) 1090–1100.
[50] L.B. Maia, I. Moura, J.J.G. Moura, Molybdenum and tungsten-containing formate dehydrogenases: aiming to inspire a catalyst for carbon dioxide utilization, Inorg. Chim. Acta 455 (2017) 350–363.
[51] D. Niks, R. Hille, Reductive activation of CO2 by formate dehydrogenases, Methods Enzymol. 613 (2018) 277–295.
[52] M.G. Rivas, M.S.P. Carepo, C.S. Mota, M. Korbas, M.-C. Durand, A.T. Lopes, C. D. Brondino, A.S. Pereira, G.N. George, A. Dolla, J.J.G. Moura, I. Moura, Molybdenum induces the expression of a protein containing a new heterometallic Mo-Fe cluster in Desulfovibrio alaskensis, Biochemistry 48 (2009) 873–882.

[53] P. Zanello, The competition between chemistry and biology in assembling iron–sulfur derivatives. Molecular structures and electrochemistry. Part III. {[Fe2S2](Cys)3(X)} (X = asp, Arg, his) and {[Fe2S2](Cys)2(his)2} proteins, Coord. Chem. Rev. 306 (2016) 420–442.

[54] J.N. Butt, S.E.J. Fawcett, J. Breton, A.J. Thomson, F.A. Armstrong, Electrochemical potential and pH dependences of [3Fe-4S] ↔ [M3Fe-4S] cluster transformations (M = Fe, Zn, co, and cd) in ferredoxin III from desulfovibrio africanus and detection of a cluster with M = Pb, J. Am. Chem. Soc. 119 (1997) 9729–9737.

[55] R.C. Conover, J.B. Park, M.W.W. Adams, M.K. Johnson, Formation and properties of an iron-nickel sulfide (NiFe3S4) cluster in Pyrococcus furiosus ferredoxin, J. Am. Chem. Soc. 112 (1990) 4562–4564.

[56] K.K. Surerus, E. Munck, I. Moura, J.J.G. Moura, J. LeGall, Evidence for the formation of a ZnFe3S4 cluster in Desulfovibrio gigas ferredoxin II, J. Am. Chem. Soc. 109 (1987) 3805–3807.

[57] K. Brown, K. Djinovic-Carugo, T. Haltia, I. Cabrito, M. Saraste, J.J. Moura, I. Moura, M. Tegoni, C. Cambillau, Revisiting the catalytic CuZ cluster of nitrous oxide (N2O) reductase, J. Biol. Chem. 275 (2000) 41133–41136.

[58] P. Hanzelmann, H. Dobbek, L. Gremer, R. Huber, O. Meyer, The effect of intracellular molybdenum in Hydrogenophaga pseudoflava on the crystallographic structure of the seleno-molybdo-iron-sulfur flavoenzyme carbon monoxide dehydrogenase, J. Mol. Biol. 301 (2000) 1221–1235.

[59] H. Dobbek, L. Gremer, R. Kiefersauer, R. Huber, O. Meyer, Catalysis at a dinuclear [CuSMo(==O)OH] cluster in a CO dehydrogenase resolved at 1.1-a resolution, Proc. Natl. Acad. Sci. U. S. A. 99 (2002) 15971–15976.

[60] M. Shanmugam, J. Wilcoxen, D. Habel-Rodriguez, G.E. Cutsail 3rd, M.L. Kirk, B. M. Hoffman, R. Hille, (13)C and (63,65)cu ENDOR studies of CO dehydrogenase from Oligotropha carboxidovorans. Experimental evidence in support of a copper-carbonyl intermediate, J. Am. Chem. Soc. 135 (2013) 17775–17782.

[61] R. Hille, S. Dingwall, J. Wilcoxen, The aerobic CO dehydrogenase from Oligotropha carboxidovorans, J. Biol. Inorg. Chem. 20 (2015) 243–251.

[62] M. Resch, H. Dobbek, O. Meyer, Structural and functional reconstruction in situ of the [CuSMoO2] active site of carbon monoxide dehydrogenase from the carbon monoxide oxidizing eubacterium Oligotropha carboxidovorans, J. Biol. Inorg. Chem. 10 (2005) 518–528.

[63] B.W. Stein, M.L. Kirk, Orbital contributions to CO oxidation in Mo-cu carbon monoxide dehydrogenase, Chem. Commun. 50 (2014) 1104–1106.

[64] B.K. Maiti, J.J.G. Moura, Diverse biological roles of the tetrathiomolybdate anion, Coord. Chem. Rev. 429 (2021), 213635.

[65] D. Sippel, M. Rohde, J. Netzer, C. Trncik, J. Gies, K. Grunau, I. Djurdjevic, L. Decamps, S.L.A. Andrade, O. Einsle, A bound reaction intermediate sheds light on the mechanism of nitrogenase, Science 359 (2018) 1484–1489.

[66] H. Dobbek, V. Svetlitchnyi, L. Gremer, R. Huber, O. Meyer, Crystal structure of a carbon monoxide dehydrogenase reveals a [Ni-4Fe-5S] cluster, Science 293 (2001) 1281–1285.

[67] B. Srour, S. Gervason, B. Monfort, B. D'Autréaux, Mechanism of iron–sulfur cluster assembly: in the intimacy of iron and sulfur encounter, Inorganics 8 (2020) 55, https://doi.org/10.3390/inorganics8100055.

[68] K.A. Black, P.C. Dos Santos, Shared-intermediates in the biosynthesis of thio-cofactors: mechanism and functions of cysteine desulfurases and sulfur acceptors, Biochim. Biophys. Acta 2015 (1853) 1470–1480.

[69] S. Leimkühler, M. Bühning, L. Beilschmidt, Shared sulfur mobilization routes for tRNA thiolation and molybdenum cofactor biosynthesis in prokaryotes and eukaryotes, Biomolecules 7 (2017) 5.

[70] A. Marquet, Enzymology of carbon-sulfur bond formation, Curr. Opin. Chem. Biol. 5 (2001) 541–549.

[71] H. Beinert, Iron-sulfur proteins: ancient structures, still full of surprises, J. Biol. Inorg. Chem. 5 (2000) 2–15.

[72] V.D. Paul, R. Lill, Biogenesis of cytosolic and nuclear iron-sulfur proteins and their role in genome stability, Biochim. Biophys. Acta 2015 (1853) 1528–1539.

[73] H. Beinert, R.H. Holm, E. Munck, Iron-sulfur clusters: nature's modular, multipurpose structures, Science 277 (1997) 653–659.

[74] W. Martin, M.J. Russell, On the origins of cells: a hypothesis for the evolutionary transitions from abiotic geochemistry to chemoautotrophic prokaryotes, and from prokaryotes to nucleated cells, Philos. Trans. R. Soc. Lond. Ser. B Biol. Sci. 358 (2003) 59–83.

[75] R. Malkin, J.C. Rabinowitz, The reconstitution of clostridial ferredoxin, Biochem. Biophys. Res. Commun. 23 (1966) 822–827.

[76] R. Lill, U. Mühlenhoff, Maturation of iron-sulfur proteins in eukaryotes: mechanisms, connected processes, and diseases, Annu. Rev. Biochem. 77 (2008) 669–700.

[77] R. Lill, Function and biogenesis of iron-Sulphur proteins, Nature 460 (2009) 831–838.

[78] T.L. Stemmler, E. Lesuisse, D. Pain, Andrew Dancis, Frataxin and mitochondrial FeS cluster biogenesis, J. Biol. Chem. 285 (2010) 26737–26743.

[79] R. Lill, B. Hoffmann, S. Molik, A.J. Pierik, N. Rietzschel, O. Stehling, M. A. Uzarska, H. Webert, C. Wilbrecht, U. Mühlenhoff, The role of mitochondria in cellular iron-sulfur protein biogenesis and iron metabolism, Biochim. Biophys. Acta 2012 (1823) 1491–1508.

[80] T.A. Rouault, Biogenesis of iron-sulfur clusters in mammalian cells: new insights and relevance to human disease, Dis. Model. Mech. 5 (2012) 155–164.

[81] L. Zheng, R.H. White, V.L. Cash, R.F. Jack, D.R. Dean, Cysteine desulfurase activity indicates a role for NIFS in metallocluster biosynthesis, Proc. Natl. Acad. Sci. U. S. A. 90 (1993) 2754–2758.

[82] W. Fu, R.F. Jack, T.V. Morgan, D.R. Dean, M.K. Johnson, nifU gene product from Azotobacter vinelandii is a homodimer that contains two identical [2Fe-2S] clusters, Biochemistry 33 (1994) 13455–13463.

[83] Y. Takahashi, U. Tokumoto, A third bacterial system for the assembly of iron-sulfur clusters with homologs in archaea and plastids, J. Biol. Chem. 277 (2002) 28380–28383.

[84] L. Zheng, R.H. White, V.L. Cash, D.R. Dean, Mechanism for the desulfurization of L-cysteine catalyzed by the nifS gene product, Biochemistry 3 (1994) 4714–4720.

[85] L. Zheng, V.L. Cash, D.H. Flint, D.R. Dean, Assembly of iron-sulfur clusters. Identification of an iscSUA-hscBA-fdx gene cluster from Azotobacter vinelandii, J. Biol. Chem. 273 (1998) 13264–13272.

[86] F.W. Outten, M.J. Wood, F.M. Munoz, G. Storz, The SufE protein and the SufBCD complex enhance SufS cysteine desulfurase activity as part of a sulfur transfer pathway for Fe-S cluster assembly in *Escherichia coli*, J. Biol. Chem. 278 (2003) 45713–45719.

[87] H. Mihara, N. Esaki, Bacterial cysteine desulfurases: their function and mechanisms, Appl. Microbiol. Biotechnol. 60 (2002) 12–23.

[88] R. Nakamura, M. Hikita, S. Ogawa, Y. Takahashi, T. Fujishiro, Snapshots of PLP-substrate and PLP-product external aldimines as intermediates in two types of cysteine desulfurase enzymes, FEBS J. 287 (2020) 1138–1154.

[89] K. Li, W.-H. Tong, R.M. Hughes, T.A. Rouault, Roles of the mammalian cytosolic cysteine desulfurase, ISCS, and scaffold protein, ISCU, in iron-sulfur cluster assembly, J. Biol. Chem. 281 (2006) 12344–12351.

[90] Y. Hu, M.W. Ribbe, Biosynthesis of the metalloclusters of nitrogenases, Annu. Rev. Biochem. 85 (2016) 455–483.

[91] S. Burén, E. Jiménez-Vicente, C. Echavarri-Erasun, L.M. Rubio, Biosynthesis of nitrogenase cofactors, Chem. Rev. 120 (2020) 4921–4968.

[92] M.M. Wuebbens, K.V. Rajagopalan, Mechanistic and mutational studies of *Escherichia coli* molybdopterin synthase clarify the final step of molybdopterin biosynthesis, J. Biol. Chem. 278 (2003) 14523–14532.

[93] G. Schwarz, R.R. Mendel, Molybdenum cofactor biosynthesis and molybdenum enzymes, Annu. Rev. Plant Biol. 57 (2006) 623–647.

[94] J.N. Daniels, M.M. Wuebbens, K.V. Rajagopalan, H. Schindelin, Crystal structure of a molybdopterin synthase-precursor Z complex: insight into its sulfur transfer mechanism and its role in molybdenum cofactor deficiency, Biochemistry 47 (2008) 615–626.

[95] J.A. Santamaria-Araujo, V. Wray, G. Schwarz, Structure and stability of the molybdenum cofactor intermediate cyclic pyranopterin monophosphate, J. Biol. Inorg. Chem. 17 (2012) 113–122.

[96] B.K. Maiti, L. Maia, K. Pal, B. Pakhira, T. Aviles, I. Moura, S.R. Pauleta, J. L. Nunez, A.C. Rizzi, C.D. Brondino, S. Sarkar, J.J.G. Moura, One electron reduced square planar bis(benzene-1,2-dithiolato) copper dianionic complex and redox switch by O2/HO•, Inorg. Chem. 53 (2014) 12799–12808.

[97] R.R. Mendel, S. Leimkühler, The biosynthesis of the molybdenum cofactors, J. Biol. Inorg. Chem. 20 (2015) 337–347.

[98] J. Krausze, C. Probst, U. Curth, J. Reichelt, S. Saha, D. Schafflick, D.W. Heinz, R. R. Mendel, T. Kruse, Dimerization of the plant molybdenum insertase Cnx1E is required for synthesis of the molybdenum cofactor, Biochem. J. 474 (2017) 163–178.

[99] R.R. Mendel, S. Leimkühler, Molybdenum cofactor biosynthesis, in: R. Hille, C. Schulzke, M.L. Kirk (Eds.), Molybdenum and Tungsten Enzymes: Biochemistry, RSC Metallobiology Series No. 5 vol. Chap 3, The Royal Society of Chemistry, Cambridge, 2017, pp. 100–116.

[100] J. Krausze, T.W. Hercher, D. Zwerschke, M.L. Kirk, W. Blankenfeldt, R.R. Mendel, T. Kruse, The functional principle of eukaryotic molybdenum insertases, Biochem. J. 475 (2018) 1739–1753.

[101] S. Leimkühler, The biosynthesis of the molybdenum cofactors in *Escherichia coli*, Environ. Microbiol. 22 (2020) 2007–2026.

[102] M.A. Hasnat, A. Zupok, J.J. Olas, B. Mueller-Roeber, S. Leimkühler, A-type carrier proteins are involved in [4Fe-4S] cluster insertion into the radical S-Adenosylmethionine protein MoaA for the synthesis of active molybdoenzymes, J. Bacteriol. (2021), https://doi.org/10.1128/JB.00086-21.

[103] T. Palmer, C.L. Santini, C. Iobbi-Nivol, D.J. Eaves, D.H. Boxer, G. Giordano, Involvement of the narJ and mob gene products in distinct steps in the biosynthesis of the molybdoenzyme nitrate reductase in *Escherichia coli*, Mol. Microbiol. 20 (1996) 875–884.

[104] M.W. Lake, C.A. Temple, K.V. Rajagopalan, H. Schindelin, The crystal structure of the Escherichia coli MobA protein provides insight into molybdopterin guanine dinucleotide biosynthesis, J. Biol. Chem. 275 (2000) 40211–40217.

[105] C.A. Temple, K.V. Rajagopalan, Mechanism of assembly of the Bis(Molybdopterin guanine dinucleotide)molybdenum cofactor in Rhodobacter sphaeroides dimethyl sulfoxide reductase, J. Biol. Chem. 275 (2000) 40202–40210.

[106] C.E. Stevenson, F. Sargent, G. Buchanan, T. Palmer, D.M. Lawson, Crystal structure of the molybdenum cofactor biosynthesis protein MobA from Escherichia coli at near-atomic resolution, Structure 8 (2000) 1115–1125.

[107] M. Neumann, G. Mittelstädt, F. Seduk, C. Iobbi-Nivol, S. Leimkühler, MocA is a specific cytidylyltransferase involved in molybdopterin cytosine dinucleotide biosynthesis in Escherichia coli, J. Biol. Chem. 284 (2009) 21891–21898.

[108] M. Neumann, F. Seduk, C. Iobbi-Nivol, S. Leimkühler, Molybdopterin dinucleotide biosynthesis in Escherichia coli: identification of amino acid residues of molybdopterin dinucleotide transferases that determine specificity for binding of guanine or cytosine nucleotides, J. Biol. Chem. 286 (2011) 1400–1408.

[109] S. Reschke, K.G.V. Sigfridsson, P. Kaufmann, N. Leidel, S. Horn, K. Gast, C. Schulzke, M. Haumann, S. Leimkühler, Identification of a bis-molybdopterin intermediate in molybdenum cofactor biosynthesis in *Escherichia coli*, J. Biol. Chem. 288 (2013) 29736–29745.

[110] C. Iobbi-Nivol, S. Leimkühler, Molybdenum enzymes, their maturation and molybdenum cofactor biosynthesis in Escherichia coli, Biochem. Bipphys. Acta 2013 (1827) 1086–1101.
[111] M. Lehrke, S. Rump, T. Heidenreich, J. Wissing, R.R. Mendel, F. Bittner, Identification of persulfide-binding and disulfide-forming cysteine residues in the NifS-like domain of the molybdenum cofactor sulfurase ABA3 by cysteine-scanning mutagenesis, Biochem. J. 441 (2012) 823–832.
[112] V. Anantharaman, L. Aravind, MOSC domains: ancient, predicted sulfur-carrier domains, present in diverse metal-sulfur cluster biosynthesis proteins including molybdenum cofactor sulfurases, FEMS Microbiol. Lett. 207 (2002) 55–61.
[113] F. Bittner, M. Oreb, R.R. Mendel, ABA3 is a molybdenum cofactor sulfurase required for activation of aldehyde oxidase and xanthine dehydrogenase in Arabidopsis thaliana, J. Biol. Chem. 276 (2001) 40381–40384.
[114] T. Heidenreich, S. Wollers, R.R. Mendel, F. Bittner, Characterization of the NifS-like domain of ABA3 from Arabidopsis thaliana provides insight into the mechanism of molybdenum cofactor sulfuration, J. Biol. Chem. 280 (2005) 4213–4218.
[115] S. Wollers, T. Heidenreich, M. Zarepour, D. Zachmann, C. Kraft, Y.D. Zhao, R. R. Mendel, F. Bittner, Binding of sulfurated molybdenum cofactor to the C-terminal domain of ABA3 from Arabidopsis thaliana provides insight into the mechanism of molybdenum cofactor sulfuration, J. Biol. Chem. 283 (2008) 9642–9650.
[116] H. Peretz, M.S. Naamati, D. Levartovsky, A. Lagziel, E. Shani, I. Horn, H. Shalev, D. Landau, Identification and characterization of the first mutation (Arg776Cys) in the C-terminal domain of the human molybdenum cofactor sulfurase (HMCS) associated with type II classical xanthinuria, Mol. Gen. Metabol. 91 (2007) 23–29.
[117] R.R. Mendel, R. Hansch, Molybdoenzymes and molybdenum cofactor in plants, J. Exp. Bot. 53 (2002) 1689–1698.
[118] L.J. Giles, C. Ruppelt, J. Yang, R.R. Mendel, F. Bittner, M.L. Kirk, Molybdenum site structure of MOSC family proteins, Inorg. Chem. 53 (2014) 9460–9462.
[119] M. Neumann, W. Stöcklein, A. Walburger, A. Magalon, S. Leimkühler, Identification of a Rhodobacter capsulatus L-cysteine desulfurase that sulfurates the molybdenum cofactor when bound to XdhC and before its insertion into xanthine dehydrogenase, Biochemistry 46 (2007) 9586–9595.
[120] S. Leimkühler, W. Klipp, Role of XDHC in molybdenum cofactor insertion into xanthine dehydrogenase of Rhodobacter capsulatus, J. Bacteriol. 181 (1999) 2745–2751.
[121] S. Leimkühler, S. Angermüller, G. Schwarz, R.R. Mendel, W. Klipp, Activity of the molybdopterin-containing xanthine dehydrogenase of Rhodobacter capsulatus can be restored by high molybdenum concentrations in a moeA mutant defective in molybdenum cofactor biosynthesis, J. Bacteriol. 181 (1999) 5930–5939.
[122] M. Neumann, M. Schulte, N. Jünemann, W. Stöcklein, S. Leimkühler, Rhodobacter capsulatus XdhC is involved in molybdenum cofactor binding and insertion into xanthine dehydrogenase, J. Biol. Chem. 281 (2006) 15701–15708.
[123] M. Neumann, W. Stöcklein, S. Leimkühler, Transfer of the molybdenum cofactor synthesized by Rhodobacter capsulatus MoeA to XdhC and MobA, J. Biol. Chem. 282 (2007) 28493–28500.
[124] M. Neumann, S. Leimkühler, The role of system-specific molecular chaperones in the maturation of molybdoenzymes in bacteria, Biochem. Res. Int. 2011 (2011), 850924.
[125] S. Leimkühler, O.N. Lemair, C. Iobbi-Nivol, Bacterial molybdoenzymes chaperons, assembly and insertion, in: R. Hille, C. Schulzke, M.L. Kirk (Eds.), Molybdenum and Tungsten Enzymes: Biochemistry, RSC Metallobiology Series No. 5 vol. Chap 4, The Royal Society of Chemistry, Cambridge, 2017, pp. 117–142.
[126] R. Thome, A. Gust, R. Toci, R. Mendel, F. Bittner, A. Magalon, A. Walburger, A sulfurtransferase is essential for activity of formate dehydrogenases in *Escherichia coli*, J. Biol. Chem. 287 (2012) 4671–4678.
[127] N. Böhmer, T. Hartmann, S. Leimkühler, The chaperone FdsC for Rhodobacter capsulatus formate dehydrogenase binds the bis-molybdopterin guanine dinucleotide cofactor, FEBS Lett. 588 (2014) 531–537.
[128] P. Arnoux, C. Ruppelt, F. Oudouhou, J. Lavergne, M.I. Siponen, R. Toci, R. R. Mendel, F. Bittner, D. Pignol, A. Magalon, A. Walburger, Sulphur shuttling across a chaperone during molybdenum cofactor maturation, Nat. Commun. 6 (2015) 6148.
[129] P. Schrapers, T. Hartmann, R. Kositzki, H. Dau, S. Reshke, C. Schulzke, S. Leimkühler, M. Haumann, Sulfido and cysteine ligation changes at the molybdenum cofactor during substrate conversion by formate dehydrogenase (FDH) from Rhodobacter capsulatus, Inorg. Chem. 54 (2015) 3260–3271.
[130] N. Schwanhold, C. Iobbi-Nivol, A. Lehmann, S. Leimkühler, Same but different: comparison of two system-specific molecular chaperones for the maturation of formate dehydrogenases, PLoS One 13 (2018), e0201935.
[131] L.B. Maia, J.J.G. Moura, I. Moura, Molybdenum and tungsten-dependent formate dehydrogenases, J. Biol. Inorg. Chem. 20 (2015) 287–309.
[132] C.F. Nielsen, L. Lange, A.S. Meyer, Classification and enzyme kinetics of formate dehydrogenases for biomanufacturing via CO2 utilization, Biotechnol. Adv. 37 (2019), 107408.
[133] N. Kato, Formate dehydrogenase from methylotrophic yeasts, Methods Enzymol. 188 (1990) 459–462.
[134] C. Vinals, E. Depiereux, E. Feytmans, Prediction of structurally conserved regions of D-specific hydroxy acid dehydrogenases by multiple alignment with formate dehydrogenase, Biochem. Biophys. Res. Commun. 192 (1993) 182–188.
[135] V.O. Popov, V.S. Lamzin, NAD + −dependent formate dehydrogenase, Biochem. J. 301 (1994) 625–643.
[136] E.V. Filippov, K.M. Polyakov, T.V. Tikhonova, T.N. Stekhanova, K.M. Boiko, K. O. Popov, Structure of a new crystal modification of the bacterial NAD-dependent formate dehydrogenase with a resolution of 2.1 Å, Crystallogr. Rep. 50 (2005) 796–800.
[137] K. Schirwitz, A. Schmidt, V.S. Lamzin, High resolution structures of formate dehydrogenase from Candida boidinii, Protein Sci. 16 (2007) 1146–1156.
[138] I.G. Shabalin, K.M. Polyakov, V.I. Tishkov, V.O. Popov, Atomic resolution crystal structure of NAD(+)-dependent formate dehydrogenase from bacterium moraxella Sp. C-1, Acta Nat 1 (2009) 89–93.
[139] A.A. Alekseeva, S.S. Savin, V.I. Tishkov, NAD (+) -dependent formate dehydrogenase from plants, Acta Nat. 3 (2011) 38–54.
[140] Q. Guo, L. Gakhar, K. Wickersham, K. Francis, A. Vardi-Kilshtain, D.T. Major, C. M. Cheatum, A. Kohen, Structural and kinetic studies of formate dehydrogenase from candida boidinii, Biochemistry 55 (2016) 2760–2771.
[141] L.G. Ljungdahl, H.G. Wood, Total synthesis of acetate from CO2 by heterotrophic bacteria, Annu. Rev. Microbiol. 23 (1969) 515–538.
[142] R.K. Thauer, CO(2)-reduction to formate by NADPH. The initial step in the total synthesis of acetate from CO(2) in Clostridium thermoaceticum, FEBS Lett. 27 (1972) 111–115.
[143] P.A. Scherer, R.K. Thauer, Purification and properties of reduced ferredoxin: CO2 oxidoreductase from Clostridium pasteurianum, a molybdenum iron-sulfur-protein, Eur. J. Biochem. 85 (1978) 125–135.
[144] C. Costa, M. Teixeira, J. LeGall, J.J.G. Moura, I. Moura, Formate dehydrogenase from Desulfovibrio desulfuricans ATCC 27774: isolation and spectroscopic characterization of the active sites, J. Biol. Inorg. Chem. 2 (1997) 198–208.
[145] J.C. Boyington, V.N. Gladyshev, S.V. Khangulov, T. Stadtman, P.D. Sun, Crystal structure of formate dehydrogenase H: catalysis involving Mo, molybdopterin, selenocysteine and an Fe4S4 cluster, Science 275 (1997) 1305–1308.
[146] S.W. Ragsdale, The eastern and western branches of the Wood/Ljungdahl pathway: how the east and west were won, BioFactors 6 (1997) 3–11.
[147] S.V.V. Khangulov, V.N. GLadyshev, G.S. Dismukes, T.C. Stadtman, Selenium-containing formate dehydrogenase H from *Escherichia coli*: a molybdenum enzyme that catalyzes formate oxidation without oxygen transfer, Biochemistry 37 (1998) 3518–3528.
[148] M.J. Almendra, C.D. Brondino, O. Gavel, A.S. Pereira, P. Tavares, S. Bursakov, R. Duarte, J. Caldeira, J.J. Moura, I. Moura, Purification and characterization of a tungsten-containing formate dehydrogenase from *Desulfovibrio gigas*, Biochemistry 38 (1999) 16366–16372.
[149] H. Raaijmakers, S. Teixeira, J.M. Dias, M.J. Almendra, C.D. Brondino, I. Moura, J. J. Moura, M.J. Romão, Tungsten-containing formate dehydrogenase from Desulfovibrio gigas: metal identification and preliminary structural data by multi-wavelength crystallography, J. Biol. Inorg. Chem. 6 (2001) 398–404.
[150] M. Jormakka, S. Törnroth, B. Byrne, S. Iwata, Molecular basis of proton motive force generation: structure of formate dehydrogenase-N, Science 2295 (2002) 1863–1868.
[151] H. Raaijmakers, S. Macieira, J.M. Dias, S. Texierira, S. Bursakov, R. Huber, J.J. G. Moura, I. Moura, M.J. Romão, Gene sequence and the 1.8Å crystal structure of the tungsten-containing formate dehydrogenase from Desulfovibrio gigas, Structure 10 (2002) 1261–1272.
[152] K. Bagramyan, A. Trchounian, Structural and functional features of formate hydrogen lyase, enzyme of mixed-acid fermentation in *Escherichia coli*, Biochem. Mosc. 68 (2003) 1159–1163.
[153] H. Wang, R.P. Gunsalus, Coordinate regulation of the Escherichia coli formate dehydrogenase fdnGHI and fdhF genes in response to nitrate, nitrite and fomate: roles fro NarL and NarP, J. Bacteriol. 185 (2003) 5076–5085.
[154] J.S.-C. Liou, D.L. Balkwill, G.R. Drake, R.S. Tanner, Clostridium carboxidivorans sp. nov., a solvent-producing clostridium isolated from an agricultural settling lagoon, and reclassification of the acetogen Clostridium scatologenes strain SL1 as Clostridium drakei sp. nov, Int. J. Syst. Evol. Microbiol. 55 (2005) 2085–2091.
[155] H.C.A. Raaijmakers, M.J. Romão, Formate-reduced E coli formate dehydrogenase H: the reinterpretation of the crystal structure suggests a new reaction mechanism, J. Biol. Inorg. Chem. 11 (2006) 849–854.
[156] M. Rivas, P. Gonzalez, C.D. Brondino, J.J.G. Moura, I. Moura, EPR characterization of the molybdenum(V) forms of formate dehydrogenase from Desulfovibrio desulfuricans ATCC 27774 upon formate reduction, J. Inorg. Biol. 101 (2007) 1617–1622.
[157] S.W. Ragsdale, E. Pierce, Acetogenesis and the Wood-Ljungdahl pathway of CO(2) fixation, Biochim. Biophys. Acta 1784 (2008) 1873–1898.
[158] G. Bruant, M.-J. Levesque, C. Peter, S.R. Guiot, L. Masson, Genomic analysis of carbon monoxide utilization and butanol production by Clostridium carboxidivorans strain P7, PLoS One 5 (2010), e13033.
[159] D. Paul, F.W. Austin, T. Arick, S.M. Bridges, S.C. Burgess, Y.S. Dandass, M. L. Lawrence, Genome sequence of the solvent-producing bacterium Clostridium carboxidivorans strain P7T, J. Bacteriol. 192 (2010) 5554–5555.
[160] S.M. Silva, C. Pimentel, F.M.A. Valente, C. Rodrigues-Pousada, I.A.C. Pereira, Tungsten and molybdenum regulation of formate dehydrogenase expression in Desulfovibrio vulgaris hildenborough, J. Bacteriol. 193 (2011) 2908–2916.
[161] S.M. Silva, I. Pacheco, I.A.C. Pereira, Electron transfer between periplasmic formate dehydrogenase and cytochromes c in Desulfovibrio desulfuricans ATCC 27774, J. Biol. Inorg. Chem. 17 (2012) 831–838.
[162] K. Trchounian, A. Poladyan, A. Vassilian, A. Trchounian, Multiple and reversible hydrogenases for hydrogen production by *Escherichia coli*: dependence on fermentation substrate, pH and the F(0)F(1)-ATPase, Crit. Rev. Biochem. Mol. Biol. 47 (2012) 236–249.
[163] S.M. da Silva, J. Voordouw, C. Leião, M. Martins, G. Voordouw, I.A.C. Pereira, Function of formate dehydrogenases in Desulfovibrio vulgaris hildenborough energy metabolism, Microbiology 159 (2013) 1760–1769.

[164] A. Alissandratos, H.K. Kim, H.K. Matthews, J.E. Hennessey, A. Philbrook, C. J. Easton, Clostridium carboxidovorans strain P7T recombinant formate dehydrogenase catalyzes reduction of CO2 to formate, Appl. Environ. Micorobiol. 79 (2013) 741–744.

[165] K. Schuchmann, V. Müller, Direct and reversible hydrogenation of CO2 to formate by a bacterial carbon dioxide reductase, Science 342 (2013) 1382–1385.

[166] J.S. McDowall, G.J. Murphy, M. Haumann, T. Palmer, F.A. Armstrong, F. Sargent, Bacterial formate hydrogenlyase complex, Proc. Natl. Acad. Sci. U. S. A. 111 (2014) E3948–E3956.

[167] J.S. Mcdowall, M.C. Hjersing, T. Palmer, F. Sargent, Dissection and engineering of the *Escherichia Coli* formate hydrogenlyase complex, FEBS Lett. 589 (2015) 3141–3147.

[168] M. Martins, M. Mourato, F.O. Morais-Silva, C. Rodrigues-Pousada, G. Voordouw, J.D. Wall, I.A.C. Pereira, Electron transfer pathways of formate-driven H2 production in Desulfovibrio, Appl. Microbiol. Biotechnol. 100 (2016) 8135–8146.

[169] C. Pinske, F. Sargent, Exploring the directionality of *Escherichia Coli* formate hydrogenlyase: a membrane-bound enzyme capable of fixing carbon dioxide to organic acid, Microbiol. Open 5 (2016) 721–737.

[170] F.M. Schwarz, K. Schuchmann, V. Müller, Hydrogenation of CO2 at ambient pressure catalyzed by a highly active thermostable biocatalyst, Biotechnol. Biofuels 11 (2018) 237.

[171] V. Müller, New horizons in acetogenic conversion of one-carbon substrates and biological hydrogen storage, Trends Biotechnol. 37 (2019) 1344–1354.

[172] M.C. Schoelmerich, V. Müller, Energy conservation by a hydrogenase-dependent chemiosmotic mechanism in an ancient metabolic pathway, Proc. Natl. Acad. Sci. U. S. A. 116 (13) (2019 Mar 26) 6329–6334.

[173] A.R. Oliveira, C. Mota, C. Mourato, R.M. Domingos, M.F.A. Santos, D. Gesto, B. Guigliarelli, T. Santos-Silva, M.J. Romão, I.A.C. Pereira, Toward the mechanistic understanding of enzymatic CO2 reduction, ACS Catal. 10 (2020) 3844–3856.

[174] I. Sánchez-Andrea, I.A. Guedes, B. Hornung, S. Boeren, C.E. Lawson, D.Z. Sousa, A. Bar-Even, N.J. Claassens, A.J.M. Stams, The reductive glycine pathway allows autotrophic growth of *Desulfovibrio desulfuricans*, Nat. Commun. 11 (2020) 5090.

[175] T. Young, D. Niks, S. Hakopian, T.K. Tam, X. Yu, R. Hille, G.M. Blaha, Crystallographic and kinetic analyses of the FdsBG subcomplex of the cytosolic formate dehydrogenase FdsABG from *Cupriavidus necator*, J. Biol. Chem. 295 (2020) 6570–6585.

[176] C. Radon, G. Mittelstädt, B.R. Duffus, J. Bürger, T. Hartmann, T. Mielke, C. Teutloff, S. Leimkühler, P. Wendler, Cryo-EM structures reveal intricate Fe-S cluster arrangement and charging in *Rhodobacter capsulatus* formate dehydrogenase, Nat. Commun. 11 (2020) 1912.

[177] D. Litty, V. Müller, Acetogenic bacteria for biotechnological applications, in: J.J. G. Moura, I. Moura, L.B. Maia (Eds.), Enzymes for Solving Humankind's Problems Chap 4, Springer, Cham, 2021, pp. 109–132.

[178] M. Meneghello, A.R. Oliveira, A. Jacq-Bailly, I.A.C. Pereira, C. Léger, V. Fourmond, Formate dehydrogenases reduce CO2 rather than HCO3–: an electrochemical demonstration, Angew. Chem. Int. Ed. Eng. 60 (2021) 9964–9967.

[179] P.A. Bertram, M. Karrasch, R.A. Schmitz, R. Böcher, S.P.J. Albracht, R.K., Thauer, formylmethanofuran dehydrogenases from methanogenic Archaea. Substrate specificity, EPR properties and reversible inactivation by cyanide of the molybdenum or tungsten iron-sulfur proteins, Eur. J. Biochem. 220 (1994) 477–484.

[180] A. Hochheimer, R. Hedderich, R.K. Thauer, The formylmethanofuran dehydrogenase isozymes in Methanobacterium wolfeii and Methanobacterium terhmoautotrophicum: induction of the molybdenum isozyme by molybdate and constitutive synthesis of the tungsten isozyme, Arch. Microbiol. 170 (1998) 389–393.

[181] L.M. de Poorter, W.G. Geerts, A.P. Theuvenet, J.T. Keltjens, Bioenergetics of the formyl-methanofuran dehydrogenase and heterodisulfide reductase reactions in *Methanothermobacter thermautotrophicus*, Eur. J. Biochem. 270 (2003) 66–75.

[182] T. Wagner, U. Ermler, S. Shima, The methanogenic CO2 reducing-and-fixing enzyme is bifunctional and contains 46 [4Fe-4S] clusters, Science 354 (2016) 114–117.

[183] D. Niks, J. Duvvuru, M. Escalona, R. Hille, Spectroscopic and kinetic properties of the molybdenum-containing, NAD + −dependent formate dehydrogenase from Ralstonia eutropha, J. Biol. Chem. 291 (2016) 1162–1174.

[184] L. Maia, L. Fonseca, I. Moura, J.J.G. Moura, Reduction of carbon dioxide by a molybdenum-containing formate dehydrogenase: a kinetic and mechanistic study, J. Am. Chem. Soc. 138 (2016) 8834–8846.

[185] E.I. Stiefel, Proposed molecular mechanism for the action of molybedenum in enzymes: coupled proton and electron transfer, Proc. Natl. Acad. Sci. U. S. A. 70 (1973) 988–992.

[186] E.I. Stiefel, The coordination and bioinorganic chemistry of molybdenum, Prog. Inorg. Chem. 22 (1977) 1–223.

[187] A. Rajapakshe, R.A. Snyder, A.V. Astashkin, P. Bernardson, D.J. Evans, C. G. Young, D.H. Evans, J.H. Enemark, Insights into the nature of Mo(V) species in solution: modeling catalytic cycles for molybdenum enzymes, Inorg. Chim. Acta 362 (2009) 4603–4608.

[188] X. Yu, D. Niks, A. Mulchandani, R. Hille, Efficient reduction of CO2 by the molybdenum-containing formate dehydrogenase from *Cupriavidus necator* (*Ralstonia eutropha*), J. Biol. Chem. 292 (2017) 16872–16879.

[189] L.M. Walker, V. Li, D. Niks, R. Hille, S.J. Elliott, Deconvolution of reduction potentials of formate dehydrogenase from *Cupriavidus necator*, J. Biol. Inorg. Chem. 24 (2018) 889–898.

[190] X. Yu, D. Niks, X. Ge, H. Liu, R. Hille, A. Mulchandani, Synthesis of formate from CO2 gas catalyzed by an O2-tolerant NAD-dependent formate dehydrogenase and glucose dehydrogenase, Biochemistry 58 (2019) 1861–1868.

[191] R. Hille, Molybdenum-containing hydroxylases, Arch. Biochem. Biophys. 433 (2005) 107.

[192] R. Hille, Structure and function of xanthine oxidoreductase, Eur. J. Inorg. Chem. 1913 (2006).

[193] R. Hille, T. Nishino, F. Bittner, Molybdenum enzymes in higher organisms, Coord. Chem. Rev. 255 (2011) 1179.

[194] K. Okamoto, T. Kusano, T. Nishino, Chemical nature and reaction mechanisms of the molybdenum cofactor of xanthine oxidoreductase, Curr. Pharm. Des. 19 (2013) 2606–2614.

[195] G.M. Montero-Moran, M. Li, E. Rendon-Huerta, F. Jourdan, D.J. Lowe, A. W. Stumpff-Kane, M. Feig, C. Scazzocchio, R.P. Hausinger, Purification and characterization of the FeII- and alpha-ketoglutarate-dependent xanthine hydroxylase from *aspergillus nidulans*, Biochemistry 46 (2007) 5293–5304.

[196] Y. Zhang, V.N. Gladyshev, Molybdoproteomes and evolution of molybdenum utilization, J. Mol. Biol. 379 (2008) 881–899.

[197] Y. Zhang, S. Rump, V.N. Gladyshev, Comparative genomics and evolution of molybdenum utilization, Coord. Chem. Rev. 255 (2011) 1206–1217.

[198] N.V. Gladyshev, Y. Zhang, Abundance, ubiquity and evolution of molybdoenzymes, in: R. Hille, C. Schulzke, M.L. Kirk (Eds.), Molybdenum and Tungsten Enzymes: Biochemistry, RSC Metallobiology Series No. 5 vol. Chap 2, The Royal Society of Chemistry, Cambridge, 2017, pp. 81–99.

[199] T.M. Millar, C.R. Stevens, N. Benjamin, R. Eisenthal, R. Harrison, D.R. Blake, Xanthine oxidoreductase catalyses the reduction of nitrates and nitrite to nitric oxide under hypoxic conditions, FEBS Lett. 427 (1998) 225–228.

[200] Z. Zhang, D. Naughton, P.G. Winyard, N. Benjamin, D.R. Blake, M.C. Symons, Generation of nitric oxide by a nitrite reductase activity of xanthine oxidase: a potential pathway for nitric oxide formation in the absence of nitric oxide synthase activity, Biochem. Biophys. Res. Commun. 249 (1998) 767–772.

[201] H.L.J. Godber, J.J. Doel, G.P. Sapkota, D.R. Blake, C.R. Stevens, R. Eisenthal, R. Harrison, Reduction of nitrite to nitric oxide catalyzed by xanthine oxidoreductase, J. Biol. Chem. 275 (2000) 7757–7763.

[202] H. Li, A. Samouilov, X. Liu, J.L. Zweier, Characterization of the magnitude and kinetics of xanthine oxidase-catalyzed nitrite reduction. Evaluation of its role in nitric oxide generation in anoxic tissue, J. Biol. Chem. 276 (2001) 24482–24489.

[203] H. Li, A. Samouilov, X. Liu, J.L. Zweier, Characterization of the effects of oxygen on xanthine oxidase-mediated nitric oxide formation, J. Biol. Chem. 279 (2004) 16939–16946.

[204] H. Li, H. Cui, T.K. Kundu, W. Alzawahra, J.L. Zweier, Nitric oxide production from nitrite occurs primarily in tissues not in the blood: critical role of xanthine oxidase and aldehyde oxidase, J. Biol. Chem. 283 (2008) 17855–17863.

[205] H. Li, T.K. Kundu, J.L. Zweier, Characterization of the magnitude and mechanism of aldehyde oxidase-mediated nitric oxide production from nitrite, J. Biol. Chem. 284 (2009) 33850–33858.

[206] L.B. Maia, V. Pereira, L. Mira, J.J.G. Moura, Nitrite reductase activity of rat and human xanthine oxidase, xanthine dehydrogenase, and aldehyde oxidase: evaluation of their contribution to NO formation in vivo, Biochemistry 54 (2015) 685–710.

[207] L.B. Maia, J.J.G. Moura, Nitrite reduction by molybdoenzymes: a new class of nitric oxide-forming nitrite reductases, J. Biol. Inorg. Chem. 20 (2015) 403–433.

[208] F.O. Gomes, L. Maia, C. Delerue-Matos, I. Moura, J.J.G. Moura, S. Morais, Third-generation electrochemical biosensor based on nitric oxide reductase immobilized in a multiwalled carbon nanotubes/1-n-butyl-3-methylimidazolium tetrafluoroborate nanocomposite for nitric oxide detection, Sensors Actuators B Chem. 285 (2019) 445–452.

[209] F.O. Gomes, L.B. Maia, J.A. Loureiro, J.J.G. Moura, S. Morais, Biosensor for direct bioelectrocatalysis detection of nitric oxide using nitric oxide reductase incorporated in carboxylated single-walled carbon nanotubes/lipidic 3 bilayer nanocomposite, Bioelectrochemistry 127 (2019) 76–86.

[210] L. Maia, J.J.G. Moura, Putting xanthine oxidoreductase and aldehyde oxidase on the NO metabolism map: nitrite reduction by molybdoenzymes, Redox Biol. 19 (2018) 274–289.

[211] S. Pardue, G.K. Kolluru, X. Shen, S.E. Lewis, C.B. Saffle, E.E. Kelley, C.G. Kevil, Hydrogen sulfide stimulates xanthine oxidoreductase conversion to nitrite reductase and formation of NO, Redox Biol. 34 (2020), 101447.

[212] D.N. Granger, G. Rutili, J.M. McCord, Role of superoxide radicals in feline intestine ischemia, Gastroenterology 81 (1981) 22.

[213] J.M. McCord, Oxygen derived free radicals in post ischemic tissue injury, N. Engl. J. Med. 312 (1985) 159–163.

[214] C.S. Lieber, Biochemical and molecular basis of alcohol induced injury to liver and other tissues, N. Engl. J. Med. 319 (1988) 1639.

[215] J.L. Zweier, P. Kuppusamy, G.A. Lutty, Measurement of endothelial cell free radical generation: evidence for a central mechanism of free radical injury in postischemic tissues, Proc. Natl. Acad. Sci. U. S. A. 85 (1988) 4046.

[216] A.I. Cederbaum, Role of lipid peroxidation and oxidative stress in alcohol toxicity, Free Radic. Biol. Med. 7 (1989) 537.

[217] S. Kato, T. Kawase, J. Alderman, N. Inatomi, C. Lieber, Role of xanthine oxidase in ethanol-induced lipid peroxidation in rats, Gastroenterology 98 (1990) 203.

[218] R. Nordmann, C. Ribière, H. Rouach, Implications of free radical mechanisms in ethanol-induced cellular injury, Free Radic. Biol. Med. 12 (1992) 219.

[219] L.S. Terada, J.J. Dormish, P.F. Shanley, J.A. Leff, B.O. Anderson, J.E. e Repine, Circulating xanthine oxidase mediates lung neutrophil sequestration after intestinal ischemia-reperfusion, Am. J. Phys. 263 (1992) L394–L401.

[220] J.L. Zweier, R. Broderick, P. Kuppusamy, S. Thompson-Gorman, G.A. Lutty, Determination of the mechanism of free radical generation in human aortic endothelial cells exposed to anoxia and reoxygenation, J. Biol. Chem. 269 (1994) 24156.
[221] A. Weinbroum, V.G. Nielsen, S. Tan, S. Gelman, S. Matalon, K.A. Skinner, E. Bradley Jr., D.A. Parks, Liver ischemia-reperfusion increases pulmonary permeability in rat: role of circulating xanthine oxidase, Am. J. Phys. 268 (1995) G988.
[222] R. Harrison, Human xanthine oxidoreductase: in search of a function, Biochem. Soc. Trans. 25 (1997) 786.
[223] T. Nishino, S. Nakanishi, K. Okamoto, J. Mizushima, H. Hori, T. Iwasaki, T. Nishino, K. Ichimori, H. Nakazawa, Conversion of xanthine dehydrogenase into oxidase and its role in reperfusion injury, Biochem. Soc. Trans. 25 (1997) 783.
[224] R.M. Wright, J.E. Repine, The human molybdenum hydroxylase gene family: co-conspirators in metabolic free-radical generation and disease, Biochem. Soc. Trans. 25 (1997) 799.
[225] K.B. Beckman, B.N. Ames, The free radical theory of aging matures, Physiol. Rev. 78 (1998) 547–581.
[226] H. Suzuki, F.A. Delano, D.A. Parks, N. Jamshidi, D.N. Granger, H. Ishii, M. Suematsu, B.W. Zweifach, G.W. Schmid-Schonbein, Xanthine oxidase activity associated with arterial blood pressure in spontaneously hypertensive rats, Proc. Natl. Acad. Sci. U. S. A. 95 (1998) 4754.
[227] R.M. Wright, J.L. McManaman, J.E. Repine, Alcohol-induced breast cancer: a proposed mechanism, Free Radic. Biol. Med. 26 (1999) 348.
[228] R. Harrison, Structure and function of xanthine oxidoreductase: where are we now? Free Radic. Biol. Med. 33 (2002) 774.
[229] F. Stirpe, M. Ravaioli, M.G. Battelli, S. Musiani, G.L. Grazi, Xanthine oxidoreductase activity in human liver disease, Am. J. Gastroenterol. 97 (2002) 2079.
[230] D. Wu, A.I. Cederbaum, Alcohol, oxidative stress, and free radical damage, Alcohol Res. Health 27 (2003) 277.
[231] C.E. Berry, J.M. Hare, Xanthine oxidoreductase and cardiovascular disease: molecular mechanisms and pathophysiological implications, J. Physiol. 555 (2004) 589.
[232] C. Hesberg, R. Haensch, R.R. Mendel, F. Bittner, Tandem orientation of duplicated xanthine dehydrogenase genes from Arabidopsis thaliana: differential gene expression and enzyme activities, J. Biol. Chem. 279 (2004) 13547–13554.
[233] L. Maia, A. Vala, L. Mira, NADH oxidase activity of rat liver xanthine dehydrogenase and xanthine oxidase: contribution for damage mechanisms, Free Radic. Res. 39 (2005) 979–986.
[234] Z. Yesbergenova, G. Yang, E. Oron, D. Soffer, R. Flur, M. Sagi, The plant Mo-hydroxylases aldehyde oxidase and xanthine dehydrogenase have distinct reactive oxygen species signatures and are induced by drought and abscisic acid, Plant J. 42 (2005) 862–876.
[235] E.E. Kelley, T. Hock, N.K. Khoo, G.R. Richardson, K.K. Johnson, P.C. Powell, G. I. Giles, A. Agarwal, J.R. Lancaster Jr., M.M., Moderate hypoxia induces xanthine oxidoreductase activity in arterial endothelial cells, Tarpey, free Radic, Biol. Med. 40 (2006) 952–959.
[236] L. Maia, R.O. Duarte, A. Ponces-Freire, J.J.G. Moura, L. Mira, NADH oxidase activity of rat and human liver xanthine oxidoreductase: potential role in superoxide production, J. Biol. Inorg. Chem. 12 (2007) 777–787.
[237] M. Zarepour, K. Kaspari, S. Stagge, R. Rethmeier, R.R. Mendel, F. Bittner, Xanthine dehydrogenase AtXDH1 from Arabidopsis thaliana is a potent producer of superoxide anions via its NADH oxidase activity, Plant Mol. Biol. 72 (2010) 301–310.
[238] D.M. Small, J.S. Coombes, N. Bennett, D.W. Johnson, G.C. Gobe, Oxidative stress, anti-oxidant therapies and chronic kidney disease, Nephrology 17 (2012) 311.
[239] M.M. Bachschmid, S. Schildknecht, R. Matsui, R. Zee, D. Haeussler, R.A. Cohen, D. Pimental, B. Loo, Vascular aging: chronic oxidative stress and impairment of redox signaling-consequences for vascular homeostasis and disease, Ann. Med. 45 (2013) 17.
[240] N. Cantu-Medellin, E.E. Kelley, Xanthine oxidoreductase-catalyzed reactive species generation: a process in critical need of reevaluation, Redox Biol. 1 (2013) 353–358.
[241] N.R. Madamanchi, M.S. Runge, Redox signaling in cardiovascular health and disease, Free Radic. Biol. Med. 61 (2013) 473.
[242] E.E. Kelley, A new paradigm for XOR-catalyzed reactive species generation in the endothelium, Pharmacol. Rep. 67 (2015) 669–674.
[243] T. Nishino, K. Okamoto, Mechanistic insights into xanthine oxidoreductase from development studies of candidate drugs to treat hyperuricemia and gout, J. Biol. Inorg. Chem. 20 (2015) 195–207.
[244] M.C. Madigan, R.M. McEnaney, A.J. Shukla, G. Hong, E.E. Kelley, M.M. Tarpey, M. Gladwin, B.S. Zuckerbraun, E. Tzeng, Xanthine oxidoreductase function contributes to normal wound healing, Mol. Med. 21 (2015) 313–322.
[245] M.G. Battelli, L. Polito, M. Bortolotti, A. Bolognesi, Xanthine oxidoreductase in drug metabolism: beyond a role as a detoxifying enzyme, Curr. Med. Chem. 23 (2016) 4027–4036.
[246] E. Garattini, M. Terao, Xanthine oxidoreductase and aldehyde oxidases, in: Comprehensive Toxicology, Third ed, Elsevier, 2017, pp. 208–232.
[247] D. Moris, M. Spartalis, E. Spartalis, G.S. Karachaliou, G.I. Karaolanis, G. Tsourouflis, D.I. Tsilimigras, E. Tzatzaki, S. Theocharis, The role of reactive oxygen species in the pathophysiology of cardiovascular diseases and the clinical significance of myocardial redox, Ann. Transl. Med. 5 (2017) 326.
[248] R. Kumar, G. Joshi, H. Kler, S. Kalra, M. Kaur, R. Arya, Toward an understanding of structural insights of xanthine and aldehyde oxidases: an overview of their inhibitors and role in various diseases, Med. Res. Rev. 38 (2018) 1073–1125.
[249] H. Terawaki, T. Hayashi, T. Murase, R. Iijima, K. Waki, Y. Tani, T. Nakamura, K. Yoshimura, S. Uchida, J.J. Kazama, Relationship between xanthine oxidoreductase redox and oxidative stress among chronic kidney disease patients, Oxid. Med. Cell Longev. 2018 (2018), 9714710, https://doi.org/10.1155/2018/9714710.
[250] B. Butts, D.A. Calhoun, T.S. Denney Jr., S.G. Lloyd, H. Gupta, K.K. GaddamK, I. Aban, S. Oparil, P.W. Sanders, R. Patel, J.F. Collawn, L.J. Dell'Italia, Plasma xanthine oxidase activity is related to increased sodium and left ventricular hypertrophy in resistant hypertension, Free Radic. Biol. Med. 134 (2019) 343–349.
[251] T. Kusano, D. Ehirchiou, T. Matsumura, V. Chobaz, S. Nasi, M. Castelblanco, A. So, C. Lavanchy, H. Acha-Orbea, T. Nishino, K. Okamoto, N. Busso, Targeted knock-in mice expressing the oxidase-fixed form of xanthine oxidoreductase favor tumor growth, Nat. Commun. 10 (2019) 4904.
[252] H.M. Schmidt, E.E. Kelley, A.C. Straub, The impact of xanthine oxidase (XO) on hemolytic diseases, Redox Biol. 21 (2019), 101072.
[253] S.S. Al-Shehri, J.A. Duley, N. Bansal, Xanthine oxidase-lactoperoxidase system and innate immunity: biochemical actions and physiological roles, Redox Biol. 34 (2020), 101524.
[254] L.G. Sanchez-Lozada, B. Rodriguez-Iturbe, E.E. Kelley, T. Nakagawa, M. Madero, D.I. Feig, C. Borghi, F. Piani, G. Cara-Fuentes, P. Bjornstad, M.A. Lanaspa, R. J. Johnson, Uric acid and hypertension: an update with recommendations, Am. J. Hypertens. 33 (2020) 583–594.
[255] M. Martorell, X. Lucas, P. Alarcón-Zapata, X. Capó, M.M. Quetglas-Llabrés, S. Tejada, A. Sureda, Targeting xanthine oxidase by natural products as a therapeutic approach for mental disorders, Curr. Pharm. Des. 27 (2021) 367–382.
[256] H.M. Schmidt, K.C. Wood, S.E. Lewis, S.A. Hahn, X.N. Williams, B. McMahon, J. J. Baust, S. Yuan, T.N. Bachman, Y. Wang, J.Y. Oh, S. Ghosh, S.F. Ofori-Acquah, J. D. Lebensburger, R.P. Patel, J. Du, D.A. Vitturi, E.E. Kelley, A.C. Straub, Xanthine oxidase drives hemolysis and vascular malfunction in sickle cell disease, Arterioscler. Thromb. Vasc. Biol. 41 (2021) 769–782.
[257] N.J. Byrne, N.S. Rajasekaran, E.D. Abel, H. Bugger, Therapeutic potential of targeting oxidative stress in diabetic cardiomyopathy, Free Radic. Biol. Med. 169 (2021) 317–342.
[258] S. Nasi, M. Castelblanco, V. Chobaz, D. Ehirchiou, A. So, I. Bernabei, T. Kusano, T. Nishino, K. Okamoto, N. Busso, Xanthine oxidoreductase is involved in chondrocyte mineralization and expressed in osteoarthritic damaged cartilage, Front. Cell Dev. Biol. 9 (2021), 612440.
[259] C. Enroth, B.T. Eger, K. Okamoto, T. Nishino, T. Nishino, E.F. Pai, Crystal structures of bovine milk xanthine dehydrogenase and xanthine oxidase: structure-based mechanism of conversion, Proc. Natl. Acad. Sci. U. S. A. 97 (2000) 10723–10728.
[260] Y. Kuwabara, T. Nishino, K. Okamoto, T. Matsumura, B.T. Eger, E.F. Pai, T. Nishino, Unique amino acids cluster for switching from the dehydrogenase to oxidase form of xanthine oxidoreductase, Proc. Natl. Acad. Sci. U. S. A. 100 (2003) 8170–8175.
[261] K. Okamoto, K. Matsumoto, R. Hille, B.T. Eger, E.F. Pai, T. Nishino, The crystal structure of xanthine oxidoreductase during catalysis: implications for reaction mechanism and enzyme inhibition, Proc. Natl. Acad. Sci. U. S. A. 101 (2004) 7931–7936.
[262] T. Nishino, K. Okamoto, Y. Kawaguchi, H. Hori, T. Matsumura, B.T. Eger, E.F. Pai, T. Nishino, Mechanism of the conversion of xanthine dehydrogenase to xanthine oxidase: identification of the two cysteine disulfide bonds and crystal structure of a non-convertible rat liver xanthine dehydrogenase mutant, J. Biol. Chem. 280 (2005) 24888–24894.
[263] T. Nishino, K. Okamoto, B.T. Eger, E.F. Pai, T. Nishino, Mammalian xanthine oxidoreductase - mechanism of transition from xanthine dehydrogenase to xanthine oxidase, FEBS J. 275 (2008) 3278–3289.
[264] H. Ishikita, B.T. Eger, K. Okamoto, T. Nishino, E.F. Pai, Protein conformational gating of enzymatic activity in xanthine oxidoreductase, J. Am. Chem. Soc. 134 (2012) 999–1009.
[265] T. Nishino, K. Okamoto, Y. Kawaguchi, T. Matsumura, B.T. Eger, E.F. Pai, T. Nishino, The C-terminal peptide plays a role in the formation of an intermediate form during the transition between xanthine dehydrogenase and xanthine oxidase, FEBS J. 282 (2015) 3075–3090.
[266] K.N. Murray, J.G. Watson, S. Chaykin, Catalysis of the direct transfer of oxygen from nicotinamide N-oxide to xanthine by xanthine oxidase, J. Biol. Chem. 241 (1966) 4798–4801.
[267] R. Hille, H. Sprecher, On the mechanism of action of xanthine oxidase: evidence in support of an oxo transfer mechanism in the molybdenum-containing hydroxylases, J. Biol. Chem. 262 (1987) 10914–10917.
[268] C.J. Doonan, A. Stockert, R. Hille, G.N. George, Nature of the catalytically labile oxygen at the active site of xanthine oxidase, J. Am. Chem. Soc. 127 (2005) 4518–4522.
[269] J.M. Pauff, J. Zhang, C.E. Bell, R. Hille, Substrate orientation in xanthine oxidase - crystal structure of enzyme in reaction with 2-hydroxy-6-methylpurine, J. Biol. Chem. 283 (2008) 4818–4824.
[270] H. Cao, J. Hall, R. Hille, Substrate orientation and specificity in xanthine oxidase: crystal structures of the enzyme in complex with indole-3-acetaldehyde and guanine, Biochemistry 53 (2014) 533–541.
[271] B.W. Stein, M.L. Kirk, Electronic structure contributions to reactivity in xanthine oxidase family enzymes, J. Biol. Inorg. Chem. 20 (2015) 183–194.
[272] P.A. Lindahl, The Ni-containing carbon monoxide dehydrogenase family: light at the end of the tunnel? Biochemistry 41 (2000) 2097–2105.

[273] C.L. Drennan, J. Heo, M.D. Sintchak, E. Schreiter, P.W. Ludden, Life on carbon monoxide: X-ray structure of Rhodospirillum rubrum Ni-Fe-S carbon monoxide dehydrogenase, Proc. Natl. Acad. Sci. U. S. A. 98 (2001) 11973–11978.
[274] T.I. Doukov, T.M. Iverson, J. Seravalli, S.W. Ragsdale, C.L. Drennan, A Ni-Fe-cu center in a bifunctional carbon monoxide dehydrogenase/acetyl-coa synthase, Science 298 (2002) 567–572.
[275] C. Darnault, A. Volbeda, E.J. Kim, P. Legrand, X. Vernède, P.A. Lindahl, J. C. Fontecilla-Camps, Ni-Zn-[Fe4-S4] and Ni-Ni-[Fe4-S4] clusters in closed and open α subunits of acetyl-CoA synthase/carbon monoxide dehydrogenase, Nat. Struct. Biol. 10 (2003) 271–279.
[276] H. Dobbek, V. Svetlitchnyi, J. Liss, O. Meyer, Carbon monoxide induced decomposition of the active site [Ni−4Fe−5S] cluster of CO dehydrogenase, J. Am. Chem. Soc. 126 (2004) 5382–5387.
[277] J. Feng, P.A. Lindahl, Effect of sodium sulfide on Ni-containing carbon monoxide dehydrogenases, J. Am. Chem. Soc. 126 (2004) 9094–9100.
[278] Z. Hu, N.J. Spangler, M.E. Anderson, J. Xia, P.W. Ludden, P.A. Lindahl, E. Münck, Nature of the C-cluster in Ni-containing carbon monoxide dehydrogenases, J. Am. Chem. Soc. 118 (1996) 830–845.
[279] J.-H. Jeoung, H. Dobbek, Carbon dioxide activation at the Ni,Fe-cluster of anaerobic carbon monoxide dehydrogenase, Science 318 (2007) 1461–1464.
[280] P.A. Lindahl, Implications of a carboxylate-bound C-cluster structure of carbon monoxide dehydrogenase†, Angew. Chem. Int. Ed. 47 (2008) 4054–4056.
[281] V.C.-C. Wang, S.T.A. Islam, M. Can, S.W. Ragsdale, F.A. Armstrong, Investigations by protein film electrochemistry of alternative reactions of nickel-containing carbon monoxide dehydrogenase, J. Phys. Chem. B 119 (2015) 13690–13697.
[282] T. Spatzal, K.A. Perez, O. Einsle, J.B. Howard, D.C. Rees, Ligand binding to the FeMo-cofactor: structures of CO-bound and reactivated nitrogenase, Science 345 (2014) 1620–1623.
[283] R.N.F. Thorneley, D.J. Lowe, in: T.G. Spiro (Ed.), Molybdenum Enzymes vol. 1, Wiley-Interscience, 1985, pp. 221–284.
[284] A.T. Thorhallsson, B. Benediktsson, R. Bjornsson, A model for dinitrogen binding in the E4 state of nitrogenase, Chem. Sci. 10 (2019) 11110–11124.
[285] L. Maia, J.J.G. Moura, How biology handles nitrite, Chem. Rev. 114 (2014) 5273–5357.
[286] W.H. Campbell, Nitrate reductase structure, function and regulation: bridging the gap between biochemistry and physiology, Annu. Rev. Plant Mol. Biol. 50 (1999) 277–303.
[287] W.H. Campbell, Structure and function of eukaryotic NAD(P)H:nitrate reductase, Cell. Mol. Life Sci. 58 (2001) 194–204.
[288] G. Xu, X. Fan, A.J. Miller, Plant nitrogen assimilation and use efficiency, Annu. Rev. Plant Biol. 63 (2012) 153.
[289] Y.Y. Wang, P.K. Hsu, Y.F. Tsay, Uptake, allocation and signaling of nitrate, Trends Plant Sci. 17 (2012) 458–467.
[290] A. Chamizo-Ampudia, E. Sanz-Luque, A. Llamas, A. Galvan, E. Fernandez, Nitrate reductase regulates plant nitric oxide homeostasis, Trends Plant Sci. 22 (2017) 163–174.
[291] M. Anas, F. Liao, K.K. Verma, M.A. Sarwar, A. Mahmood, Z.L. Chen, Q. Li, X. P. Zeng, Y. Liu, Fate of nitrogen in agriculture and environment: agronomic, eco-physiological and molecular approaches to improve nitrogen use efficiency, Biol. Res. 53 (2020) 47.
[292] R. Kishorekumar, M. Bulle, A. Wany, K.J. Gupta, An overview of important enzymes involved in nitrogen assimilation of plants, Methods Mol. Biol. 2057 (2020) 1–13.
[293] D.J. Richardson, Bacterial respiration: a flexible process for a changing environment, Microbiology 146 (2000) 551–571.
[294] L. Potter, H. Angove, D. Richardson, J. Cole, Nitrate reduction in the periplasm of gram-negative bacteria, Adv. Microb. Physiol. 45 (2001) 51–112.
[295] J.F. Stolz, P. Basu, Evolution of nitrate reductase: molecular and structural variations on a common function, ChemBioChem 3 (2002) 198–206.
[296] M.G. Bertero, R.A. Rothery, M. Palak, C. Hou, D. Lim, F. Blasco, J.H. Weiner, N.C. J. Strynadka, Insights into the respiratory electron transfer pathway from the structure of nitrate reductase a, Nat. Struct. Biol. 10 (2003) 681–687.
[297] M. Jormakka, D. Richardson, B. Byrne, S. Iwata, Architecture of NarGH reveals a structural classification of Mo-bisMGD enzymes, Structure 12 (2004) 95–104.
[298] P.G. González, C. Correia, I. Moura, C.D. Brondino, J.J.G. Moura, Bacterial nitrate reductases: molecular and biological aspects of nitrate reduction, J. Inorg. Biochem. 100 (2006) 1015–1023.
[299] R.M. Martinez-Espinosa, E.J. Dridge, M.J. Bonete, J.N. Butt, C.S. Butler, F. Sargent, D.J. Richardson, Look on the positive side! The orientation, identification and bioenergetics of 'Archaeal' membrane-bound nitrate reductases, FEMS Microbiol. Lett. 276 (2007) 129–139.
[300] M. Kern, J. Simon, Periplasmic nitrate reduction in Wolinella succinogenes: cytoplasmic NapF facilitates NapA maturation and requires the menaquinol dehydrogenase NapH for membrane attachment, Microbiology 155 (2009) 2784–2794.
[301] E.C. Lowe, S. Bydder, R.S. Hartshorne, H.L.U. Tape, E.J. Dridge, C.M. Debieux, K. Paszkiewicz, I. Singleton, R.J. Lewis, J.M. Santini, D.J. Richardson, C.S. Butler, Quinol-cytochrome c oxidoreductase and cytochrome c4 mediate electron transfer during selenate respiration in Thauera selenatis, J. Biol. Chem. 285 (2010) 18433–18442.
[302] F.O. Gomes, L.B. Maia, J.A. Loureiro, M.C. Pereira, C. Delerue-Matos, I. Moura, J. J.G. Moura, S. Morais, Biosensor for direct bioelectrocatalysis detection of nitric oxide using nitric oxide reductase incorporated in carboxylated single-walled carbon nanotubes/lipidic 3 bilayer nanocomposite, Bioelectrochem. 127 (2019) 76–86.
[303] C. Sparacino-Watkins, J.F. Stolzb, P. Basu, Nitrate and periplasmic nitrate reductases, Chem. Soc. Rev. 43 (2014) 676–706.
[304] C. Coelho, M.J. Romão, Structural and mechanistic insights on nitrate reductases, Protein Sci. 24 (2015) 1901–1911.
[305] F. Alberge, L. Espinosa, F. Seduk, L. Sylvi, R. Toci, A. Walburger, A. Magalon, Dynamic subcellular localization of a respiratory complex controls bacterial respiration, Elife. 4 (2015), e05357.
[306] P.J. González, M.G. Rivas, J.G. Moura, Structure, function and mechanisms of respiratory nitrate reductases, in: I. Moura, J.J.G. Moura, S.R. Pauleta, L. Maia (Eds.), Metalloenzymes in Denitrification: Applications and Environmental Impacts, RSC Metallobiology Series No. 9 Chap 4, The Royal Society of Chemistry, Cambridge, 2017, pp. 39–58.
[307] S. Bulot, S. Audebert, L. Pieulle, F. Seduk, E. Baudelet, L. Espinosa, M.C. Pizay, L. Camoin, A. Magalon, Clustering as a means to control nitrate respiration efficiency and toxicity in *Escherichia coli*, mBio. 10 (2019) e01832-19.
[308] S. Durand, M. Guillier, Transcriptional and post-transcriptional control of the nitrate respiration in bacteria, Front. Mol. Biosci. 8 (2021), 667758.
[309] S. Gutteridge, R.C. Bray, B.A. Notton, R.J. Fido, E.J. Hewitt, Studies by electron-paramagnetic-resonance spectroscopy of the molybdenum Centre of spinach (*Spinacia oleracea*) nitrate reductase, Biochem. J. 213 (1983) 137–142.
[310] S.P. Cramer, L.P. Solomonson, M.W.W. Adams, L.E. Mortenson, Molybdenum sites of *Escherichia coli* and *Chlorella vulgaris* nitrate reductase: a comparison by EXAFS, J. Am. Chem. Soc. 106 (1984) 1467–1471.
[311] L.P. Solomonson, M.J. Barber, W.D. Howard, J.L. Johnson, K.V. Rajagopalan, Electron paramagnetic resonance studies on the molybdenum center of assimilatory NADH:nitrate reductase from chlorella vulgaris, J. Biol. Chem. 259 (1984) 849–853.
[312] G.N. George, J.A. Mertens, W.H. Campbell, Structural changes induced by catalytic turnover at the molybdenum site of arabidopsis nitrate reductase, J. Am. Chem. Soc. 121 (1999) 9730–9737.
[313] K. Fischer, G.G. Barbier, H.J. Hecht, R.R. Mendel, W.H. Campbell, G. Schwarz, Structural basis of eukaryotic nitrate reduction: crystal structures of the nitrate reductase active site, Plant Cell 17 (2005) 1167–1179.
[314] B.J.N. Jepson, S. Mohan, T.A. Clarke, A.J. Gates, J.A. Cole, C.S. Butler, J.N. Butt, A.M. Hemmings, D.J. Richardson, Spectropotentiometric and structural analysis of the periplasmic nitrate reductase from *Escherichia coli*, J. Biol. Chem. 282 (2007) 6425–6437.
[315] B. Mintmier, J.M. McGarry, D.J. Bain, P. Basu, Kinetic consequences of the endogenous ligand to molybdenum in the DMSO reductase family: a case study with periplasmic nitrate reductase, J. Biol. Inorg. Chem. 26 (2021) 13–28.
[316] J.M. Dias, M.E. Than, A. Humm, R. Huber, G.P. Bourenkov, H.D. Bartunik, S. Bursakov, J. Calvete, J. Caldeira, C. Carneiro, J.J. Moura, I. Moura, M. J. Romão, Crystal structure of the first dissimilatory nitrate reductase at 1.9 a solved by MAD methods, Structure 7 (1999) 65–79.
[317] A. Marietou, D. Richardson, J. Cole, S. Mohan, Nitrate reduction by Desulfovibrio desulfuricans: a periplasmic nitrate reductase system that lacks NapB, but includes a unique tetraheme c-type cytochrome, NapM, FEMS Microbiol. Lett. 248 (2005) 217–225.
[318] C. Coelho, P.J. Gonzalez, J.G. Moura, I. Moura, J. Trincão, M.J. Romão, The crystal structure of Cupriavidus necator nitrate reductase in oxidized and partially reduced states, J. Mol. Biol. 408 (2011) 932–948.
[319] C. Coelho, M.J. Romão, Structural and mechanistic insights on nitrate reductases, Protein Sci. 24 (2015) 1901–1911.
[320] N.M. Cerqueira, P.J. Gonzalez, C.D. Brondino, M.J. Romao, C.C. Romao, I. Moura, J.J.G. Moura, The effect of the sixth sulfur ligand in the catalytic mechanism of periplasmic nitrate reductase, J. Comput. Chem. 30 (2009) 2466–2484.
[321] J.L.C. Duff, J.L.J. Breton, J.N. Butt, F.A. Armstrong, A.J. Thomson, Novel redox chemistry of [3Fe−4S] clusters: electrochemical characterization of the all-Fe(II) form of the [3Fe−4S] cluster generated reversibly in various proteins and its spectroscopic investigation in sulfolobus acidocaldarius ferredoxin, J. Am. Chem. Soc. 118 (1996) 8593–8603.
[322] B.K. Maiti, R.M. Almeida, J.J.G. Moura, Rubredoxins derivatives: simple Sulphur-rich coordination metal sites and its relevance for biology and chemistry, Coord. Chem. Rev. 352 (2017) 379–397.
[323] R.S. Magliozzo, B.A. McIntosh, W.V. Sweeney, Origin of the pH dependence of the midpoint reduction potential in Clostridium pasteurianum ferredoxin:oxidation state-dependent hydrogen ion association, J. Biol. Chem. 257 (1982) 3506–3509.
[324] J.L. Breton, J.L. Duff, J.N. Butt, F.A. Armstrong, S.J. George, Y. Pétillot, E. Forest, G. Schäfer, A.J. Thomson, Identification of the iron-sulfur clusters in a ferredoxin from the archaeon Sulfolobus acidocaldarius. Evidence for a reduced [3Fe-4S] cluster with pH-dependent electronic properties, Eur. J. Biochem. 233 (1995) 937–946.
[325] C. Moreno, A.L. Macedo, I. Moura, J. LeGall, J.J. Moura, Redox properties of Desulfovibrio gigas [Fe3S4] and [Fe4S4] ferredoxins and heterometal cubane-type clusters formed within the [Fe3S4] core. Square wave voltammetric studies, J. Inorg. Biochem. 53 (1994) 219–234.
[326] E.T. Smith, J.M. Blamey, Z.H. Zhou, M.W. Adams, A variable-temperature direct electrochemical study of metalloproteins from hyperthermophilic microorganisms involved in hydrogen production from pyruvate, Biochemistry 34 (1995) 7161–7169.
[327] J. Tong, B.A. Feinberg, Direct square-wave voltammetry of superoxidized [4Fe-4S]3+ aconitase and associated 3Fe/4Fe cluster interconversions, J. Biol. Chem. 269 (1994) 24920–24927.
[328] B. Shen, L.L. Martin, J.N. Butt, F.A. Armstrong, C.D. Stout, G.M. Jensen, P. J. Stephens, G.N. La Mar, C.M. Gorst, B.K. Burgess, Azotobacter vinelandii

ferredoxin I. aspartate 15 facilitates proton transfer to the reduced [3Fe-4S] cluster, J. Biol. Chem. 268 (1993) 25928–25939.
[329] F.A. Armstrong, J.N. Butt, S.J. George, E.C. Hatchikian, A.J. Thomson, Evidence for reversible multiple redox transformations of [3Fe-4S] clusters, FEBS Lett. 259 (1989) 15–18.
[330] J.N. Butt, F.A. Armstrong, J. Breton, S.J. George, A.J. Thomson, E.C. Hatchikian, Investigation of metal ion uptake reactivities of [3Fe-4S] clusters in proteins: voltammetry of co-adsorbed ferredoxin-aminocyclitol films at graphite electrodes and spectroscopic identification of transformed clusters, J. Am. Chem. Soc. 113 (1991) 6663–6670.
[331] H. Beinert, M.C. Kennedy, 19th sir Hans Krebs lecture. Engineering of protein bound iron-sulfur clusters. A tool for the study of protein and cluster chemistry and mechanism of iron-sulfur enzymes, Eur. J. Biochem. 186 (1989) 5–15.
[332] I. Moura, J.J.G. Moura, E. Munck, V. Papaefthymiou, J. LeGall, Evidence for the formation of a cobalt-iron-sulfur (CoFe3S4) cluster in Desulfovibrio gigas ferredoxin II, J. Am. Chem. Soc. 108 (1986) 349–351.
[333] K.K. Surerus, E. Munck, I. Moura, J.J.G. Moura, J. LeGall, Evidence for the formation of a ZnFe3S4 cluster in Desulfovibrio gigas ferredoxin II, J. Am. Chem. Soc. 109 (1987) 3805–3806.
[334] J.N. Butt, A. Sucheta, F.A. Armstrong, J. Breton, A.J. Thomson, E.C. Hatchikian, Binding of thallium(I) to a [3Fe-4S] cluster: evidence for rapid and reversible formation of [Tl3Fe-4S]2+ and [Tl3Fe-4S]1+ centers in a ferredoxin, J. Am. Chem. Soc. 113 (1991) 8948–8950.
[335] J.N. Butt, J. Niles, F.A. Armstrong, J. Breton, A.J. Thomson, Formation and properties of a stable 'high-potential' copper-iron-Sulphur cluster in a ferredoxin, Nat. Struct. Biol. 1 (1994) 427–433.
[336] K.K.P. Srivastava, K.K. Surerus, R.C. Conover, M.K. Johnson, J.B. Park, M.W. W. Adams, E. Munck, Moessbauer study of zinc-iron-sulfur ZnFe3S4 and nickel-iron-sulfur NiFe3S4 clusters in Pyrococcus furiosus ferredoxin, Inorg. Chem. 32 (1993) 927–936.
[337] W. Fu, J. Telser, B.M. Hoffman, E.T. Smith, M.W.W. Adams, M.G. Finnegan, R. C. Conover, M.K. Johnson, Interaction of Tl+ and Cs+ with the [Fe3S4] cluster of pyrococcus furiosus ferredoxin: investigation by resonance raman, MCD, EPR, and ENDOR spectroscopy, J. Am. Chem. Soc. 116 (1994) 5722–5729.
[338] M.G. Finnegan, R.C. Conover, J. Park, Z.H. Zhou, M.W.W. Adams, M.K. Johnson, Electronic, magnetic, redox, and ligand-binding properties of [MFe3S4] clusters (M = Zn, co, Mn) in pyrococcus furiosus ferredoxin, Inorg. Chem. 34 (1995) 5358–5369.
[339] F.A. Armstrong, Dynamic electrochemistry of iron—sulfur proteins, Adv. Inorg. Chem. 38 (1992) 117–163.
[340] A. Sucheta, R. Cammack, J. Weiner, F.A. Armstrong, Reversible electrochemistry of fumarate reductase immobilized on an electrode surface. Direct voltammetric observations of redox centers and their participation in rapid catalytic electron transport, Biochemistry 32 (1993) 5455–5465.
[341] T. Iwasaki, T. Wakagi, Y. Isogai, K. Tanaka, T. Iizuka, T. Oshima, Functional and evolutionary implications of a [3Fe-4S] cluster of the dicluster-type ferredoxin from the thermoacidophilic archaeon, Sulfolobus sp. strain 7, J. Biol. Chem. 269 (1994) 29444–29450.
[342] D. Beckett, Biotin sensing: universal influence of biotin status on transcription, Annu. Rev. Genet. 41 (2007) 443–464.
[343] D. Beckett, Biotin sensing at the molecular level, J. Nutr. 139 (2009) 167–170.
[344] A.M. Taylor, C.E. Farrar, J.T. Jarrett, 9-Mercaptodethiobiotin is formed as a competent catalytic intermediate by *Escherichia coli* biotin synthase, Biochemistry 47 (2008) 9309–9317.
[345] A.M. Taylor, S. Stoll, R.D. Britt, J.T. Jarrett, Reduction of the [2Fe–2S] cluster accompanies formation of the intermediate 9 Mercaptodethiobiotin in Escherichia coli biotin synthase, Biochemistry 50 (2011) 7953–7963.
[346] J.B. Broderick, B.R. Duffus, K.S. Duschene, E.M. Shepard, Radical S-adenosylmethionine enzymes, Chem. Rev. 114 (2014) 4229–4317.
[347] W.E. Broderick, B.M. Hoffman, J.B. Broderick, Mechanism of radical initiation in the radical S-Adenosyl-l-methionine superfamily, Acc. Chem. Res. 51 (2018) 2611–2619.
[348] S. Impano, H. Yang, E.M. Shepard, R. Swimley, A. Pagnier, W.E. Broderick, B. M. Hoffman, J.B. Broderick, S-Adenosyl-l-ethionine is a catalytically competent analog of S-Adenosyl-l-methione (SAM) in the radical SAM enzyme HydG, Angew. Chem. Int. Ed. Eng. 60 (2021) 4666–4672.
[349] N.B. Ugulava, B.R. Gibney, J.T. Jarrett, Biotin synthase contains two distinct iron-sulfur cluster binding sites: chemical and spectroelectrochemical analysis of iron-sulfur cluster interconversions, Biochemistry 40 (2001) 8343–8351.
[350] N.B. Ugulava, K.K. Surerus, J.T. Jarrett, Evidence from Mössbauer spectroscopy for distinct [2Fe-2S](2+) and [4Fe-4S](2+) cluster binding sites in biotin synthase from *Escherichia coli*, J. Am. Chem. Soc. 124 (2002) 9050–9051.
[351] F. Berkovitch, Y. Nicolet, J.T. Wan, J.T. Jarrett, C.L. Drennan, Crystal structure of biotin synthase, an S-adenosylmethionine-dependent radical enzyme, Science 303 (2004) 76–79.
[352] N.D. Lanz, S.J. Booker, Auxiliary iron-sulfur cofactors in radical SAM enzymes, Biochim. Biophys. Acta 2015 (1853) 1316–1334.
[353] F. Escalettes, D. Florentin, B.T.S. Bui, D. Lesage, A. Marquet, Biotin synthase mechanism: evidence for hydrogen transfer from the substrate into deoxyadenosine, J. Am. Chem. Soc. 121 (1999) 3571–3578.
[354] L. Tao, T.A. Stich, C.J. Fugate, J.T. Jarrett, R.D. Britt, EPR-derived structure of a paramagnetic intermediate generated by biotin synthase BioB, J. Am. Chem. Soc. 140 (2018) 12947–12963.
[355] N.B. Ugulava, C.J. Sacanell, J.T. Jarrett, Spectroscopic changes during a single turnover of biotin synthase: destruction of a [2Fe-2S] cluster accompanies sulfur insertion, Biochemistry 40 (2001) 8352–8358.
[356] O. Kabil, R. Banerjee, Redox biochemistry of hydrogen sulfide, J. Biol. Chem. 285 (2010) 21903–21907.
[357] H. Kimura, Hydrogen sulfide: from brain to gut, Antioxid. Redox Signal. 12 (2010) 1111–1123.
[358] O. Kabil, R. Banerjee, Enzymology of H2S biogenesis, decay and signaling, Antioxid. Redox Signal. 20 (2014) 770–782.
[359] O. Kabil, N. Motl, R. Banerjee, H2S and its role in redox signaling, Biochim. Biophys. Acta 2014 (1844) 1355–1366.
[360] T.M. Hildebrandt, M.K. Grieshaber, Three enzymatic activities catalyze the oxidation of sulfide to thiosulfate in mammalian and invertebrate mitochondria, FEBS J. 275 (2008) 3352–3361.
[361] S. Singh, D. Padovani, R.A. Leslie, T. Chiku, R. Banerjee, Relative contributions of cystathionine beta-synthase and gamma-cystathionase to H2S biogenesis via alternative trans-sulfuration reactions, J. Biol. Chem. 284 (2009) 22457–22466.
[362] N. Shibuya, M. Tanaka, M. Yoshida, Y. Ogasawara, T. Togawa, K. Ishii, H. Kimura, 3-Mercaptopyruvate Sulfurtransferase produces hydrogen sulfide and bound Sulfane sulfur in the brain, Antioxid. Redox Signal. 11 (2009) 703–714.
[363] O. Kabil, R. Banerjee, Characterization of patient mutations in human persulfide dioxygenase (ETHE1) involved in H2S catabolism, J. Biol. Chem. 287 (2012) 44561–44567.
[364] O. Kabil, V. Vitvitsky, R. Banerjee, Sulfur as a signaling nutrient through hydrogen sulfide, Annu. Rev. Nutr. 34 (2014) 171–205.
[365] V. Vitvitsky, P.K. Yadav, A. Kurthen, R. Banerjee, Sulfide oxidation by a noncanonical pathway in red blood cells generates thiosulfate and polysulfides, J. Biol. Chem. 290 (2015) 8310–8320.
[366] S.J. Riedl, G.S. Salvesen, The apoptosome: signalling platform of cell death, Nat. Rev. Mol. Cell Biol. 8 (2007) 405–413.
[367] S. Yoshikawa, A. Shimada, Reaction mechanism of cytochrome c oxidase, Chem. Rev. 115 (2015) 1936–1989.
[368] M. Wikström, K. Krab, V. Sharma, Oxygen activation and energy conservation by cytochrome c oxidase, Chem. Rev. 118 (2018) 2469–2490.
[369] L.Chr. Petersen, The effect of inhibitors on the oxygen kinetics of cytochrome c oxidase, Biochim. Biophys. Acta 460 (1977) 299–307.
[370] P. Nicholls, The effect of sulphide on cytochrome aa3. Isosteric and allosteric shifts of the reduced alpha-peak, Biochim. Biophys. Acta 396 (1975) 24–35.
[371] D. Keilin, Cytochrome and respiratory enzymes, Proc. R. Soc. Lond. B 104 (1929) 206–252.
[372] B.C. Hill, P. Nicholls, Cytochrome c reduction by cysteine plus copper: a pseudosubstrate system for cytochrome c oxidase, Can. J. Biochem. 58 (1980) 499–503.
[373] B.C. Hill, T.C. Woon, P. Nicholls, J. Peterson, C. Greenwood, A.J. Thomson, Interactions of sulphide and other ligands with cytochrome c oxidase. An electron-paramagnetic-resonance study, Biochem. J. 224 (1984) 591–600.
[374] P. Nicholls, Inhibition of cytochrome c oxidase by Sulphide, Biochem. Soc. Trans. 3 (1975) 316–319.
[375] P. Nicholls, J.K. Kim, Sulphide as an inhibitor and electron donor for the cytochrome c oxidase system, Can. J. Biochem. 60 (1982) 613–623.
[376] P. Nicholls, J.K. Kim, Oxidation of sulphide by cytochrome aa3, Biochim. Biophys. Acta 637 (1981) 312–320.
[377] B.B. Ríos-González, E.M. Román-Morales, R. Pietri, J. López-Garriga, Hydrogen sulfide activation in hemeproteins: the sulfheme scenario, J. Inorg. Biochem. 133 (2014) 78–86.
[378] D.W. Kraus, J.B. Wittenberg, Hemoglobins of the Lucina pectinata/bacteria symbiosis. I. Molecular properties, kinetics and equilibria of reactions with ligands, J. Biol. Chem. 265 (1990) 16043–16053.
[379] S. Fernandez-Alberti, D.E. Bacelo, R.C. Binning Jr., J. Echave, M. Chergui, J. Lopez-Garriga, Sulfide-binding hemoglobins: effects of mutations on active-site flexibility, Biophys. J. 91 (2006) 1698–1709.
[380] F. Hoppe-Seyler, Ueber die chemischen und optischen Eigenschaften des Blutfarbstoffs Zentbl, Med. Wiss. 1 (1983) 433–434.
[381] D. Keilin, On the combinations of methæmoglobin with H2S, Proc. R. Soc. Lond. B 113 (1933) 393–404.
[382] P. Nicholls, The formation and properties of sulphmyoglobin and sulphcatalase, Biochem. J. 81 (1961) 374–383.
[383] S.V. Evans, B.P. Sishta, A.G. Mauk, G.D. Brayer, Three-dimensional structure of cyanomet-sulfmyoglobin C, Proc. Natl. Acad. Sci. U. S. A. 91 (1994) 4723–4726.
[384] E.A. Johnson, The reversion to haemoglobin of sulphhaemoglobin and its coordination derivatives, Biochim. Biophys. Acta 207 (1970) 30–40.
[385] H.O. Michel, A study of sulfhemoglobin, J. Biol. Chem. 126 (1938) 323–348.
[386] C. Szabó, Hydrogen sulphide and its therapeutic potential, Nat. Rev. Drug Discov. 6 (2007) 917–935.
[387] T.L. Guidotti, Occupational exposure to hydrogen sulfide in the sour gas industry: some unresolved issues, Int. Arch. Occup. Environ. Health 66 (1994) 153–160.
[388] J. Dupouy, F. Petureau, J.-L. Montastruc, S. Oustric, B. Degano, A rare cause of cyanosis: Sulphaemoglobinaemia related to thiocolchicoside (Miorel), Rev. Mal. Respir. 27 (2010) 80–83.
[389] W.D. Jesús-Bonilla, J.E. Cortés-Figueroa, F.A. Souto-Bachiller, L. Rodríguez, J. López-Garriga, Formation of compound I and compound II ferryl species in the reaction of hemoglobin I from Lucina pectinata with hydrogen peroxide, Arch. Biochem. Biophys. 390 (2001) 304–308.
[390] J.A. Berzofsky, J. Peisach, W.E. Blumberg, Sulfheme proteins. I. Optical and magnetic properties of sulfmyoglobin and its derivatives, J. Biol. Chem. 246 (1971) 3367–3377.
[391] M.J. Chatfield, G.N.L. Mar, R.J. Kauten, Proton NMR characterization of isomeric sulfmyoglobins: preparation, interconversion, reactivity patterns, and structural features, Biochemistry 26 (1987) 6939–6950.

[392] E. Román-Morales, R. Pietri, B. Ramos-Santana, S.N. Vinogradov, A. Lewis-Ballester, J. López-Garriga, Structural determinants for the formation of sulfhemeprotein complexes, Biochem. Biophys. Res. Commun. 400 (2010) 489–492.
[393] B.L. Predmore, D.J. Lefer, G. Gojon, Hydrogen sulfide in biochemistry and medicine, Antioxid. Redox Signal. 17 (2012) 119–140.
[394] J.F. Cerda-Colón, E. Silfa, J. López-Garriga, Unusual rocking freedom of the heme in the hydrogen sulfide-binding hemoglobin from lucinapectinata, J. Am. Chem. Soc. 120 (1998) 9312–9317.
[395] M. Rizzi, J.B. Wittenberg, A. Coda, P. Ascenzi, M. Bolognesi, Structural bases for sulfide recognition in Lucina pectinata hemoglobin I, J. Mol. Biol. 258 (1996) 1–5.
[396] T. Bostelaar, V. Vitvitsky, J. Kumutima, B.E. Lewis, P.K. Yadav, T.C. Brunold, M. Filipovic, N. Lehnert, T.L. Stemmler, R. Banerjee, Hydrogen sulfide oxidation by myoglobin, J. Am. Chem. Soc. 138 (2016) 8476–8488.
[397] V. Vitvitsky, P.K. Yadav, S. An, J. Seravalli, U.-S. Cho, R. Banerjee, Structural and mechanistic insights into hemoglobin-catalyzed hydrogen sulfide oxidation and the fate of polysulfide products, J. Biol. Chem. 292 (2017) 5584–5592.
[398] J.H. Laity, B.M. Lee, P.E. Wright, Zinc finger proteins: new insights into structural and functional diversity, Curr. Opin. Struct. Biol. 11 (2001) 39–46.
[399] K. Zhao, S. Li, L. Wu, C. Lai, G. Yang, Hydrogen sulfide represses androgen receptor transactivation by targeting at the second zinc finger module, J. Biol. Chem. 289 (2014) 20824–20835.
[400] E. Schoenmakers, P. Alen, G. Verrijdt, B. Peeters, G. Verhoeven, W. Rombauts, F. Claessens, Differential DNA binding by the androgen and glucocorticoid receptors involves the second Zn-finger and a C-terminal extension of the DNA-binding domains, Biochem. J. 341 (1999) 515–521.
[401] B.L. Vallee, D.S. Auld, Active zinc binding sites of zinc metalloenzymes, Matrix Suppl. 1 (1992) 5–19.
[402] B.L. Vallee, D.S. Auld, Functional zinc-binding motifs in enzymes and DNA-binding proteins, Faraday Discuss. Chem. Soc. 93 (1992) 47–65.
[403] B.L. Vallee, D.S. Auld, Active-site zinc ligands and activated H2O of zinc enzymes, Proc. Natl. Acad. Sci. U. S. A. 87 (1990) 220–224.
[404] B.L. Vallee, D.S. Auld, New perspectives on zinc biochemistry: cocatalytic sites in multi-zinc enzyme, Biochemistry 32 (1993) 6493–6500.
[405] H. Laggner, M. Hermann, H. Esterbauer, M.K. Muellner, M. Exner, B.M. Gmeiner, S. Kapiotis, The novel gaseous vasorelaxant hydrogen sulfide inhibits angiotensin-converting enzyme activity of endothelial cells, J. Hypertens. 25 (2007) 2100–2104.
[406] M.R. Filipovic, J. Zivanovic, B. Alvarez, R. Banerjee, Chemical biology of H 2 S signaling through Persulfidation, Chem. Rev. 118 (2018) 1253–1337.
[407] K. Zhao, S. Li, L. Wu, C. Lai, G. Yang, Hydrogen sulfide represses androgen receptor transactivation by targeting at the second zinc finger module, J. Biol. Chem. 289 (2014) 20824–20835.
[408] M. Lange, K. Ok, G.D. Shimberg, B. Bursac, L. Markó, I. Ivanović-Burmazović, S.L. J. Michel, M.R. Filipovic, Direct zinc finger protein persulfidation by H2S is facilitated by Zn, Angew. Chem. Int. Ed. 58 (2019) 7997–8001.
[409] M. Bucci, A. Papapetropoulos, V. Vellecco, Z. Zhou, A. Pyriochou, C. Roussos, F. Roviezzo, V. Brancaleone, G. Cirino, Hydrogen sulfide is an endogenous inhibitor of phosphodiesterase activity, Arterioscler. Thromb. Vasc. Biol. 30 (2010) 1998–2004.
[410] F. Talaei, H.R. Bouma, M.N. Hylkema, A.M. Strijkstra, A.S. Boerema, M. Schmidt, R.H. Henning, The role of endogenous H2S formation in reversible remodeling of lung tissue during hibernation in the Syrian hamster, J. Exp. Biol. 215 (2012) 2912–2919.
[411] A. Innocenti, S. Zimmerman, J.G. Ferry, A. Scozzafava, C.T. Supuran, Carbonic anhydrase inhibitors. Inhibition of the zinc and cobalt γ-class enzyme from the archaeon Methanosarcina thermophila with anions, Bioorg. Med. Chem. Lett. 14 (2004) 3327–3331.
[412] G. Yang, H2S as a potential defense against COVID-19? Am. J. Phys. Cell Phys. 319 (2020) C244–C249.
[413] D.E.K. Sutherland, M.J. Stillman, The “magic numbers” of metallothionein, Metallomics 3 (2011) 444–463.
[414] Y. Zhang, A. Ali, Z. Jin, Y. Pei, G. Yang, Induction of cystathionine gamma-lyase expression and metallothionein-1 S-sulfhydration alleviate cadmium-induced cell death in myoblast cells, Ecotoxicol. Environ. Saf. 179 (2019) 222–231.
[415] F. Zal, E. Leize, F.H. Lallier, A. Toulmond, A.V. Dorsselaer, J.J. Childress, S-Sulfohemoglobin and disulfide exchange: the mechanisms of sulfide binding by Riftia pachyptila hemoglobins, Proc. Natl. Acad. Sci. U. S. A. 95 (1998) 8997–9002.
[416] J.F. Flores, C.R. Fisher, S.L. Carney, B.N. Green, J.K. Freytag, S.W. Schaeffer, W. E. Royer Jr., Sulfide binding is mediated by zinc ions discovered in the crystal structure of a hydrothermal vent tubeworm hemoglobin, Proc. Natl. Acad. Sci. U. S. A. 102 (2005) 2713–2718.